Title: Arabidopsis Phospholipase C3 is Involved in Lateral Root Initiation and ABA Responses in Seed Germination and Stomatal Closure

Running head: Role for Arabidopsis PLC3 in lateral root development and ABA signaling

Corresponding author: Email, t.munnik@uva.nl

Subject areas: 1) Growth and Development, 2) Environmental and Stress Responses

Number of:

- **black and white figures:** 3
- **colour figures:** 6
- **tables:** 0
- **type and number of supplementary material:** 1 Table; 11 Figures

Title: Arabidopsis Phospholipase C3 is Involved in Lateral Root Initiation and ABA Responses in Seed Germination and Stomatal Closure

Qianqian Zhang,[1,2] Ringo van Wijk,[1,2] Muhammad Shahbaz,[1#] Wendy Roels,[1] Bas van Schooten,[1] Joop E.M. Vermeer,[1,3] Xavier Zarza,[1,2] Aisha Guardia,[4] Denise Scuffi,[4] Carlos García-Mata,[4] Debabrata Laha,[5,6] Phoebe Williams,[7] Leo A.J. Willems,[8] Wilco Ligterink,[8] Susanne Hoffmann-Benning,[9] Glenda Gillaspy,[7] Gabriel Schaaf,[5,6] Michel A. Haring,[1] Ana M. Laxalt,[4] & Teun Munnik[1,2*]

[1]Swammerdam Institute for Life Sciences, section Plant Physiology, University of Amsterdam, Science Park 904, Amsterdam, 1098 XH, The Netherlands.
[2] Swammerdam Institute for Life Sciences, section Plant Cell Biology, University of Amsterdam, Science Park 904, Amsterdam, 1098 XH, The Netherlands.
[3]Dept. of Plant and Microbial Biology, University of Zürich, Zürich, Switzerland.
[4]Instituto de Investigaciones Biológicas (IIB-CONICET-UNMdP), Universidad Nacional de Mar del Plata, Mar del Plata, Argentina.
[5] Center for Plant Molecular Biology, University of Tübingen, Tübingen, Germany.
[6] Institute of Crop Science and Resource Conservation, Department of Plant Nutrition, University of Bonn, Bonn, Germany
[7]Dept. of Biochemistry, Virginia Polytechnic Institute and State University, Blacksburg, VA, USA.
[8]Lab. of Plant Physiology, Wageningen University & Research, Droevendaalsesteeg 1, 6708 PB, Wageningen, The Netherlands.
[9]Dept. of Biochemistry & Molecular Biology, Michigan State University, East Lansing, MI, USA.
[#]Current address: Dept. of Botany, University of Agriculture, Faisalabad, Pakistan.

***Corresponding author:** Email, t.munnik@uva.nl

Abbreviations: DAG, diacylglycerol or days after germination; IP_3, inositol 1,4,5-trisphosphate; IP_6, inositolhexakisphosphate and phytate; IPP, inositolpolyphosphate; PA, phosphatidic acid; PC, phosphatidylcholine; PE, phosphatidylethanolamine; PG, phosphatidylglycerol; PI, phosphatidylinositol; PIP, phosphatidylinositolphosphate; PIP_2, phosphatidylinositol 4,5-bisphosphate; PIPK, PIP 5-kinase; PLC, phospholipase C; PP-IPP, pyrophosphorylated-inositolpolyphosphate; PP2C, type 2C protein phosphatase; SnRK2, SNF1-Related kinase; SLAC1: slow anion channel 1

Abstract

Phospholipase C (PLC) is well known for its role in animal signaling, where it generates the second messengers, inositol 1,4,5-trisphosphate (IP_3) and diacylglycerol (DAG) by hydrolyzing the minor phospholipid, phosphatidylinositol 4,5-bisphosphate (PIP_2) upon receptor stimulation. In plants, PLC's role is still unclear, especially because the primary targets of these second messengers are lacking, i.e. the ligand-gated Ca^{2+} channel and protein kinase C, but also because PIP_2 levels are extremely low. Nonetheless, the Arabidopsis genome encodes 9 *PLCs*. We used a reversed-genetic approach to explore PLC's function in Arabidopsis and report here that PLC3 is required for proper root development, seed germination and stomatal opening. Two independent knock-down mutants, *plc3-2* and *plc3-3*, were found to exhibit reduced lateral root densities by 10-20%. Mutant seeds germinated slower but were less sensitive to ABA to prevent germination. Guard cells of *plc3* were also compromised in ABA-dependent stomatal closure. Promoter-GUS analyses confirmed *PLC3* expression in guard cells and germinating seeds, and revealed that the majority is expressed in vascular tissue, most likely phloem companion cells, i.e. in roots, leaves and flowers. *In vivo* $^{32}P_i$-labeling revealed that ABA stimulated the formation of PIP_2 in germinating seeds and guard cell-enriched leaf peels, which was significantly reduced in *plc3* mutants. Overexpression of *PLC3* had no effect on root system architecture or seed germination, but increased the plant's tolerance to drought. Our results provide genetic evidence for PLC's involvement in plant development and ABA signaling, and confirm earlier observations that overexpression increases drought tolerance. Potential molecular mechanisms for the above observations are discussed.

Key words: ABA, Arabidopsis, drought tolerance, lateral root formation, seed germination, stomatal closure.

Introduction

In animals, phospholipase C (PLC) plays a crucial role in cellular signalling. It is activated by hundreds of receptors, which causes the minor plasma membrane lipid, phosphatidylinositol 4,5-bisphosphate (PIP_2) to be hydrolyzed into the second messengers, inositol 1,4,5- trisphosphate (IP_3) and diacylglycerol (DAG). While IP_3 diffuses into the cytosol where it triggers the release of Ca^{2+} from an intracellular Ca^{2+} store via a ligand-gated Ca^{2+} channel, DAG remains in the plasma membrane where it recruits and activates members of the protein kinase C (PKC) family. Subsequent changes in Ca^{2+}- and phosphorylation status affect multiple protein targets and downstream cellular processes (Irvine, 2006; Michell, 2008; Balla, 2013).

Much less is clear about the PLC-signaling system in plants (Ischebeck et al. 2010; Munnik, 2014; Heilmann, 2016; Heilmann and Ischebeck 2016; Gerth et al. 2017). Initially, it was thought to be equivalent to the animal paradigm since most of the components driving the pathway were thought to be present (Munnik et al. 1997a; Stevenson et al. 2000; Meijer and Munnik, 2003;), especially when microinjected IP_3 was shown to release Ca^{2+} from an intracellular store and to induce stomatal closure (Gilroy et al. 1990; Blatt et al. 1990; Allen and Sanders, 1994; Hunt and Gray, 2001). However, 20 years later Brearley's lab provided evidence that it was not IP_3, but its subsequent conversion into IP_6 that caused these effects (Lemtiri-Chlieh et al. 2000, 2003). Similarly, not DAG but its phosphorylated product, phosphatidic acid (PA) has been emerging as the plant lipid-second messenger (Munnik, 2001; Laxalt and Munnik, 2002; Testerink and Munnik, 2005; Arisz et al. 2009; Testerink and Munnik, 2011; McLoughlin and Testerink 2013; Pokotylo et al. 2014; Munnik, 2014; Hou et al. 2016; Vermeer et al. 2017). Moreover, genome sequencing has meanwhile confirmed that flowering plants lack homologs of both IP_3 receptor and PKC (Wheeler and Brownlee, 2008; Munnik and Testerink, 2009; Munnik and Vermeer, 2010; Munnik and Nielsen, 2011; Munnik, 2014; Heilmann, 2016; Gerth et al. 2017).

That PLC is important for plants, however, has come from several studies. Silencing of *PLC1* in Arabidopsis and tobacco has indicated a role for PLC in ABA signaling in seed germination and stomatal closure, respectively (Sanchez and Chua, 2001; Hunt et al. 2003). ABA has been shown to trigger IP_6 responses minutes after application in potato guard-cell protoplasts and in duck weed turions (Lemtiri-Chlieh et al. 2000, 2003; Flores and Smart, 2000) but it is unknown whether this requires PLC. Interestingly, off the nine Arabidopsis *PLCs*, six are induced upon ABA (Hirayama et al. 1995; Tasma et al. 2008; Pokotylo et al. 2014).

PLC signaling has been linked to other plant abiotic-stress responses, including salt-, drought- (mimicked by sorbitol, mannitol or PEG) and heat stress (Liu et al. 2006a,b,c; Vermeer and Munnik, 2010; Zheng et al. 2012; Abd-El-Haliem et al. 2012; Gao et al. 2014; Munnik, 2014; Pokotylo et al. 2014). Interestingly, these stresses have also been shown to trigger an increase in PIP_2 levels (Pical et al. 1999; DeWald et al. 2001; Zonia and Munnik, 2004; van Leeuwen et al. 2007; Darwish et al. 2009; Mishkind et al. 2009). In some cases, IP_3 responses were reported but none of these studies addressed IP_6 or any of the other inositolpolyphosphates (IPPs) that are emerging as signaling molecules, i.e. IP_4,

IP_5, and the pyrophosphorylated inositolphosphates (PP-IPPs), IP_7 and IP_8 (Takahashi et al. 2001; Zonia et al. 2002; Liu, et al. 2006a,b; Zheng et al. 2012; Gillaspy 2013; Laha et al. 2015, 2016). Decreases in PIP have also been reported (Cho et al. 1993; Pical et al. 1999; DeWald et al. 2001; Vermeer et al. 2009) and theoretically, PLC could use PI4P as a substrate. In fact, PI4P and PIP_2 are hydrolyzed equally well *in vitro* but *in vivo* this is still not clear (Munnik, 2014). Overexpression of *PLC* has been shown to increase drought tolerance in maize, canola and tobacco (Wang et al. 2008; Georges et al. 2009; Tripathy et al. 2011; Nokhrina et al. 2014). The molecular mechanism for this still remains unknown (Das et al. 2005; Georges et al. 2009).

PLC has also been implicated in plant-microbe interactions (Laxalt and Munnik, 2002; Abd-El-Haliem and Joosten, 2017), both symbiotic and pathogenic (Luit et al. 2000; Hartog et al. 2003; De Jong et al. 2004). For some of these interactions, nitric oxide signaling has been shown and is required (Laxalt et al., 2007; Raho et al. 2011; Lanteri et al. 2011). Genetic evidence for PLC's role in disease resistance has been obtained for tomato (Vossen et al. 2010; Gonorazky et al. 2014, 2016) and recently for Arabidopsis PLC2 (D'Ambrosio et al. 2017).

Apart from stress, PLC signaling has also been linked to pollen tube growth (Helling et al. 2006; Dowd et al. 2006; Ischebeck etv al., 2010; Heilmann and Ischebeck, 2016) and gametophyte development (Song et al. 2008; Li et al. 2015; Di Fino et al. 2017). In *Physcomitrella, PLC1* has been shown to play a role in cytokinin- and gravity responses (Repp et al. 2004).

Arabidopsis contains 9 *PLC* genes (Tasma et al. 2009; Munnik, 2014; Pokotylo et al. 2014). So far, no developmental disorders other than the gametophyte development defects mentioned above were reported for Arabidopsis mutants, presumably due to strong genetic redundancy. Ordering T-DNA insertion mutants of various *PLC*s, we discovered that *plc3* mutants exhibited a lateral root phenotype. From there, we investigated PLC3's function further and found genetic evidence for its involvement in ABA responses in seed germination and stomatal closure, and that overexpression of *PLC3* lead to increased drought tolerance.

Results

Knock-down of *PLC3* affects lateral root density

To be able to investigate PLC3's function, two independent homozygous T-DNA insertion mutants were isolated, i.e. *plc3-2* (SALK_037453) and *plc3-3* (SALK_054406), exhibiting T-DNA inserts in exon 3 and intron 3 in the X-domain, respectively (Fig. 1A). Genotyping was verified by RT-PCR (Fig. 1B) and *PLC3* expression by Q-PCR (Fig. 1C), which showed that both insertion lines were knock-down (KD) mutants having lost ~90% of the *PLC3* transcript.

Growing seedlings on agar plates revealed that *plc3* mutants exhibited a small but significant difference in root system architecture compared to wild type (WT), i.e. shorter primary roots (5-10%), less lateral roots (~10-20%), and reduced lateral root densities (Figs. 1D, 1E).

Expression of *PLC3* during plant development

RT- and Q-PCR analyses have shown that Arabidopsis *PLC3* is expressed in all major plant tissues (Hunt et al. 2004; Tasma et al. 2008). To investigate this in more detail, *PLC3*-promotor GUS-YFP reporter lines were generated, using a *2.4 kb PLC3*-promoter fragment (*PLC3*$_{pro}$*:GUS-YFP*). Histochemical analyses revealed GUS activity in all stages of plant development, but expression was very much restricted to the vasculature, including root, shoot, cotyledons, leaves, different flower parts as well as in developing seeds (Figs. 2A-N). The trichome bases also revealed expression (Figs. 2J-K), but subsequent phenotypic analysis of WT and *plc3* trichomes revealed no differences in terms of shape or density (not shown).

Strikingly, the vascular *PLC3* expression in the main root was not homogenous. At the distal side of the maturation zone, the expression was often found to be discontinuous i.e. *'segmented'* (Figs. 2C-D; Supplemental Fig. 1). In the apical maturation zone it was continuous until the transition zone (Fig. 2F) and there was no *PLC3* expression at the root tip (Fig. 2I). Interestingly, lateral roots always emerged from a segment, but not every segment led to a lateral root (Fig. 2C, D).

To investigate the correlation between *PLC3* expression at the vasculature and lateral root formation in more detail, GUS expression was analysed in seedlings grown on agar plates positioned in a 45º angle, which forces lateral roots to specifically emerge at the curved sites (Ditengou et al. 2008). Under these conditions, less segments were found, and those present were always located at a curved position (Supplemental Fig. S2; red and blue circles) from most of which a lateral root emerged (Supplemental Fig. S2; blue circles). Moreover, every lateral root came from a segment (Supplemental Fig. S2). Interestingly, a similar discontinous, segmented pattern was found for tertiary root formation (Fig. 2E).

To obtain more detailed information about the *PLC3* expression, optical cross- and longitudinal sections were made by confocal microscopy to visualize the YFP expression. These analyses suggest that *PLC3* is specifically expressed in the phloem (Supplemental Fig. S3), which correlates with data on the eFP browser, showing predominant expression in the phloem companion cells (Winter et al. 2007).

Together, these results confirm that *PLC3* is expressed throughout the plant (Hunt et al. 2004; Tasma et al. 2008), and show that this expression is predominantly restricted to the vasculature, particularly in the phloem. Data also shows that the segmented *PLC3*-expression pattern positively correlates with lateral root formation.

PLC3 is involved in seed germination

When growing seedlings on agar plates, we observed that *plc3* mutants germinated slightly slower than WT seeds (Fig. 3A). Seeds were imbibed on ½MS plates in the dark at 4 °C for 48 h after which they were transferred to the light. After 24 h in the light, *plc3-2* and *plc3-3* mutants were found to germinate 54% and 60% less than wt, respectively, and after 28 h this difference was 17% and 34% (Fig. 3A). In the end, all seeds germinated. Subsequent analysis of *PLC3*-expression in germinating seeds revealed

GUS activity in embryo cotyledons and shoot apical meristems during testa rupture and radical emergence (Fig. 3B), confirming a role for *PLC3* in seed germination.

Since the delayed seed germination in the *plc3* mutants could have consequences for the observed difference in primary root growth, we analysed the relative root growth of mutants and WT at various days after germination. From these analyses, it became clear that the primary roots of *plc3* mutants grew with similar speed as WT. The differences in lateral root densities remained, however. (Supplemental Fig. S4).

Loss-of-*PLC3*-function results in decreased sensitivity to ABA inhibited-seed germination

To test whether the difference in seed germination was due to ABA sensitivity, germination experiments were repeated on ½MS plates ± ABA. Without ABA, *plc3* mutants germinated slower than WT as was described above (Figs. 3A, C). Addition of ABA inhibited seed germination, however, in this case the *plc3* mutants were clearly found to be less sensitive to ABA inhibition (Fig. 3C). For example, after 40 h of 1 μM ABA, 12.5% of *plc3-2* and 10.5% of *plc3-3* seeds had germinated, whereas only 2.5% of the WT seeds. These differences remained or even increased over time (Fig. 3C, left panel). Using 2 μM ABA, seed germination was stronger inhibited, but again revealed higher germination rates for both *plc3* mutants than WT (Fig. 3C, right panel).

Loss-of-*PLC3*-function results in decreased sensitivity to ABA induced-stomatal closure

Since ABA also plays a key role in guard-cell signaling (Munemasa et al. 2015), and since antisense-*PLC* expression had been shown to reduce the stomatal-closure response to ABA in *Nicotiana tabacum* (Hunt et al. 2003), we investigate the potential involvement of PLC3 in Arabidopsis guard cell-ABA responses.

First, we determined whether *PLC3* was expressed in guard cells since this was not obvious from previous histochemical analyses (Fig. 2), or from the eFP browser (Winter et al. 2007). Performing histochemical GUS analyses on epidermal-leaf peels clearly indicated *PLC3* expression in guard cells (Fig. 4A). Next, the stomatal-closure response was tested in leaf peels of WT and *plc3* mutants after treatment with different concentrations of ABA (i.e. 0, 0.1, 1 and 10 μM). In the absence of ABA, no significant differences in the stomatal aperture between WT and *plc3* mutants were found (Fig. 4B). However, with increasing concentrations of ABA, both *plc3-2* and *plc3-3* clearly exhibited reduced stomatal-closure responses (Fig. 4B). These results indicate that PLC3 plays a role in ABA sensitivity, both in seed germination and stomatal-closure. We also tested ABA on the root architecture of WT and *plc3* seedlings but found no siginicant difference (Supplemental Fig. S5)

ABA triggers PIP_2 synthesis in germinating seeds, seedlings and guard cells

Next, we analysed the phospholipid levels in response to ABA in different tissues and genotypes using *in vivo* $^{32}P_i$-labeling. First, germinating seeds were analysed. As shown in Figure 5, the ^{32}P-labeled PIP_2 levels were significantly higher in *plc3* mutants than in WT seeds, i.e. 23% and 22% for *plc3-2* and

plc3-3, respectively (Figs. 5A, B). No significant differences in PIP- or PA levels were found, nor in the structural phospholipids (Figs. 5A, B; data not shown). Upon ABA treatment, a significant increase in PIP_2 (27%) in wild-type seeds was found, which was absent from the *plc3* mutants (Fig. 5B). No significant changes in any of the other phospholipids were found for either genotype (Figs. 5A, B).

To check the lipid-signaling responses in guard cells, epidermal-leaf peels from WT and mutant leaves were used. In these peels, most of the mesophyl cells are dead while guard cells remain alive, which was checked by FDA/propidium iodide staining (not shown). In this case, the $^{32}P_i$-prelabeling was restricted to only 3 hrs as longer incubation times negatively affected the viability of the guard cells. Similar to what we observed in germinating seeds, *plc3* mutants contained slightly higher PIP_2 levels in guard cells, while the levels of PIP, PA and the structural phospholipids were the same as WT (Fig. 6; not shown). Upon ABA (15 min), a significant increase of PIP_2 was found for WT, which was lacking from the *plc3* mutants (Fig. 6). No significant differences for PIP, PA or any of the structural phospholipids were found ($P<0.05$).

Seedlings also revealed an increase in PIP_2 upon ABA treatment but this only became apparent after 30-60 min (Supplemental Figs. S6A-D). However, in this case no differences between WT and the *plc3* seedlings were observed (Supplemental Figs. S6E, F). No effect on the other phospholipids was found, nor differences between genotypes (Supplemental Figs. S6B-D, G, H).

Over-expression of *PLC3* increases drought tolerance

To test whether the reduced ABA responsiveness of guard cells in leaf peels of *plc3* mutants was detectable *in planta*, the drought tolerance of wild-type and *plc3*-mutant plants was investigated. Well-watered plants were grown on soil for 4 weeks, after which watering was stopped and subsequent survival rates were scored. However, no significant differences between WT and *plc3* mutants could be observed in three independent experiments (Supplemental Fig. S7).

In maize, canola and tobacco, overexpression of *PLC* has been shown to increase their drought tolerance (Georges et al. 2009; Wang et al. 2008; Tripathy et al. 2011). Whether this was caused by a specific, maybe yet unknown, substrate specificity of the chosen PLC or whether the canonical PLC function (i.e. hydrolysis of PIP_2) was responsible for the phenotype remains unknown. To test whether PLC3 overexpression could increase the drought tolerance of Arabidopsis, we generated transgenic plants ectopically expressing *PLC3* using the *UBQ10* promoter. Independent transgenic plants were selected from T0 to T3 and multiple homozygous lines were obtained. Two homozygous lines, *PLC3-OE9* and *PLC3-OE16* were selected for further analyses, which overexpressed *PLC3* by ~48-fold and ~20-fold, respectively (Fig. 7A). Growing these OE lines next to WT plants on soil or agar plates, no phenotype was observed. However, when their drought tolerance was analysed on four-weeks old soil grown plants, the PLC3-OE lines were found to perform better than WT (Fig. 7B), showing significantly higher survival rates in three independent experiments (Fig. 7B, C). Upon drought, the fresh weight of the WT shoot decreased by ~21%, which occurred less in *PLC3-OE9* or *PLC3-OE16* (17% and 12%, respectively; Fig. 7D). The dry weight was also higher in *PLC3-OE* lines and this was

independent of the drought treatment (Fig. 7E). When the loss-of-water in detached rosettes of 4-week old WT- and *PLC3*-OE plants was compared, the latter lost significantly less water (Fig. 7F), which was also reflected in increased values of relative water content (RWC %) of *PLC3-OE* rosettes under drought conditions (Supplemental Fig. S8).

Guard-cell responsiveness in leaf peels revealed that the stomatal aperture of *PLC3-OE*s was strongly reduced (~30%; Fig. 7G). Upon 0.1 μM ABA, stomatal closure was initiated in each genotype, but the aperture of the *PLC3-OE* lines was still significantly smaller than WT 's. Above 1 μM ABA, these differences were lost (Fig. 7G).

***PLC3*-overexpressing plants respond to osmotic stress with stronger PIP_2 responses**

To determine whether overexpression of *PLC3* caused any changes in the level of the signaling lipids, ^{32}P-labeled seedlings were treated with and without sorbitol to mimic drought stress. As shown in Figure 8, no major differences between WT and *PLC3-OE* lines were found under control conditions. However, upon sorbitol treatment, a much stronger PIP_2 response was observed in the *PLC3-OE* lines. In WT, the PIP_2 levels increased by about 300%, whereas the OE lines revealed a ~600% increase (Fig. 8B). The osmotic stress-induced decrease in PIP and increase in PA appeared to be similar between mutant and wildtype seedlings (Fig. 8B). These results suggest that *PLC3-OE* lines exhibit a more potent PIP_2 response under osmotic stress.

Discussion

In this paper, new roles for PLC in stress signaling and development have been identified. Using Arabidopsis loss-of-function mutants, we provide genetic evidence that *AtPLC3* is involved in seed germination, root development, stomatal movement and ABA signaling. The phenotypes are subtle but were consistent in two independent mutants, *plc3-2* and *plc3-3* and in different seed batches >10 years. Redundancy of any of the other 8 *PLCs,* of which several exhibit overlapping expression profiles with *PLC3* (Tasma et al. 2008) may be responsible for this. Overexpression of *PLC3* had no effect on the root architecture or seed germination but did increase the plant's tolerance to drought, as has been observed when overexpressing *PLC* in maize, tobacco and canola (Wang et al. 2008; Georges et al. 2009; Tripathy et al. 2011; Nokhrina et al. 2014). That overexpression of a single gene can increase the plant's tolerance to drought is interesting and may bare agricultural applications. Currently, we are investigating the underlying molecular mechanism of this phenotype and whether other Arabidopsis *PLCs* can achieve this too, or whether it is *PLC3*-specific.

While the above findings underline the importance of PLC in signaling plant stress and development, we still know very little of how this is achieved at the molecular level. Theoretically, there are several possibilities. Activation of PLC would produce DAG and IP_2 or IP_3, (depending on whether PIP or PIP_2 is used as substrate), and while plants lack the classical targets of the mammalian paradigm (i.e. IP_3 receptor, PKC), it is likely that the phosphorylated products, i.e. PA and higher IPPs

(incl. PP-IPPs) fulfil the second messenger function in plants. Various biological processes have been linked to these molecules and several protein targets involved in signal transduction and metabolism have been identified too (see below). In guard cells for example, ABA has been shown to induce the formation of IP_6 and to release Ca^{2+} from an intracellular (Lemtiri-Chlieh et al. 2000, 2003), so the plant PLC system could potentially achieve this. We found no changes in the basal levels of PPIs, PA or IPP in the *plc3* mutants, which is likely due to genetic and/or biochemical redundancy (Supplemental Fig. S6). Upon ABA, however, *plc3* mutants revealed enhanced PIP_2 responses, likely the result of reduced PIP_2 hydrolysis in WT cells expressing *PLC3*. Promoter-GUS analyses revealed that this may be very local, i.e in guard cells and vascular tissue, in particular the phloem companion cells (Fig. 2). This means that, independent of *PLC* redundancy, its very local expression may cause differences in PLC's substrate- and/or product levels between *plc3* and WT to be difficult to identify.

It is possible that PLC hydrolyses PIP rather than PIP_2 (Munnik, 2014). Concentrations of the latter are extremely low in the plasma membranes of plants, whereas PI4P levels are comparable to those found in mammalian cells, or even more abundant (van Leeuwen et al. 2007; Vermeer et al. 2008; Munnik, 2014; Balla, 2015; Simon et al. 2014, 2015). In order to make IP_6 out of IP_2 or IP_3, the same two inositolpolyphosphate kinases (IPKs) are involved. IPK2 is an inositol multiphosphate kinase that can phosphorylate the 3-, 5-, and 6- position of the inositol ring to produce IP_5, while IPK1 specifically phosphorylates IP_5 at the 2-position to produce IP_6. VIH2 is a recently discovered IPK that is responsible for the production of the PP-IPPs, i.e. IP_8. Like in animal- and fungi, IPPs and PP-IPPs are emerging as signaling molecules in plants too (York, 2006; Michell, 2008; Burton et al. 2009; Shears, 2009; Desai et al. 2014; Laha et al. 2015). However, plants also use IPPs to store phosphate as phytate, and even though this likely occurs in distinct cells, tissues and even organelles, it makes studying their levels extremely complex (Stevenson-Paulik et al. 2005; Munnik and Vermeer, 2010; Desai et al. 2014; Kuo et al. 2014, 2017; Laha et al., 2015, 2016).

Another function of PLC could be to attenuate PIP_2 signaling. Even though the concentration of this lipid in plants is extremely low under control conditions, during certain aspects of plant growth and development, and upon certain stresses, PIP_2 is readily produced and suggested to fulfil a second messenger function itself (Ischebeck et al. 2010; Gillaspy, 2013; Rodriguez-Villalon et al. 2015; Heilmann, 2015; 2016; Gerth et al. 2017; Zarza et al. 2017). Potential targets include proteins involved in ion transport (e.g. K^+ channels), membrane trafficking (endo/exocytosis via clathrin and Exo70) and the cytoskeleton (e.g. small G-protein, Rop) (Ischebeck et al. 2010; Gillaspy, 2013; Munnik, 2014; Heilmann, 2016). Similarly, PLC could function as an attenuator of PI4P signaling (Balla, 2013; Munnik, 2014). As far as we know, PLCs are not able to hydrolyse D3-phosphorylated inositol lipids [i.e. PI3P and $PI(3,5)P_2$] or PI5P (Balla, 2013; Munnik, 2014). Whether the newly linked PLC3 functions observed here, reflect PLC's role as second messenger producer or -attenuator (or both), remains to be established. Below, a broader perspective of our results is given and some potential molecular mechanisms are discussed.

Role for *PLC3* in seed germination

The delayed germination phenotype of *plc3* mutants (Fig. 3A) together with the promoter-GUS activity in germinating seeds (Fig. 3B), indicate a role for PLC3 in seed germination. Since ABA is known to inhibit seed germination (Nambara et al. 2010; Nakashima & Yamaguchi-Shinozaki, 2013), we investigated whether the delayed germination of *plc3* seeds was caused by hypersensitivity to ABA. Surprisingly, *plc3* mutants were found to be less sensitive to ABA (Fig. 3C). The latter results are in agreement with Sanchez & Chua (2001), who found that the ABA sensitivity of seed germination and downstream-gene expression was lost when silencing *PLC1* in Arabidopsis. Interestingly, we also found that guard cells of *plc3* mutants were less sensitive to ABA, so this could point to a more general role for PLC3 in ABA signaling (see below). At least, the above results indicate that the delayed germination rate in *plc3* mutants is not linked to ABA hypersensitivity.

PIP_2 levels were significantly higher in germinating *plc3* seeds (Fig. 5), which would be consistent with a reduction of PLC3 activity that would normally hydrolyze this lipid to produce IP_3. Unfortunately, the latter is very difficult to measure because seeds contain tiny amounts of IP_3 and huge amounts of IP_6, and they are extremely difficult to label with ^{3}H-inositol (Stevenson-Paulik et al. 2005). Seeds hardly take-up the label, and the high endogenous phytate concentration may also be the reason why young seedlings require relatively long labeling times (i.e. 4-11 days) to get some incorporation. Seeds typically store high amounts of IP_6 during their development as a source of phosphate (e.g. for DNA, ATP, membranes and sugars) and inositol (for IPPs, PPIs, and cell wall sugars), which is required for germination, and the growth and development of the seedling (Munnik and Nielsen, 2011). This 'storage' IP_6 is difficult - if not impossible - to distinguish from the IP_6 that has a 'signaling' function, even though they may be differentially localized in cells and tissues (Munnik and Vermeer, 2010; Gillaspy, 2011, 2013). During seed germination, IP_6 is rapidly broken down to IP_3 (Luo et al. 2012), which could be an alternative explanation for what has been assumed to be PLC-generated IP_3 (Munnik & Vermeer, 2010).

Raffinose Family Oligosaccharides (RFOs) is another group of molecules that links to inositol. RFOs serve as transport sugars in phloem, as storage sugars in various tissues, and as desiccation protectant in seeds (van den Ende 2013; Sengupta et al. 2015). In Arabidopsis, RFOs are required for the rapid germination of seeds in the dark (Gangl and Tenhaken, 2016). RFOs are sucrose derivatives to which a galactosyl unit is attached via galactinol. The latter is produced via UDP-galactose and *myo*-inositol by the enzyme, galactinol synthase. To make RFOs, free *myo*-inositol is required and this is predominantly formed through cyclization of glycolytic glucose 6-phosphate into inositol-3-phosphate, and subsequent dephosphorylation by inositol mono- phosphatase. Theoretically, however, inositol could be generated via dephosphorylation of PLC-generated IPPs (Munnik and Vermeer, 2010). We therefore analysed the soluble carbohydrate composition in seeds but found no significant differences

between WT and *plc3* mutants (Supplemental Fig. S9A). Of course, changes could be local and small, so it is possible differences remain unobserved.

Promoter-GUS analyses of developing seeds revealed *PLC3* expression at the chalaza (Fig. 2M), the non-micropylar end of the seed, which is likely the chalaza endosperm and/or seed coat. Nutrients from the mother plant are transported via the vascular tissue through the chalaza into the nucellus. The vascular- and chalaza expression of *PLC3* might be necessary for nutrient transport. Alternatively, PLC could be involved in the production of IP_6 for storage of essential minerals. Developing seeds store these minerals in three locations, i.e. in the protein storage vacuoles of the embryo, and transiently in the endoplasmic reticulum (ER) and vacuolar compartments of the chalaza endosperm. X-ray analysis and enzyme treatments have suggested that these minerals are stored as IP_6-salts with distinct cation (Mg, Mn, Zn, K, and Ca) composition per compartment (Otegui et al. 2002). As such, this could be another mechanism by which loss of *PLC3* redundantly affects seed germination and root development.

Role for *PLC3* in lateral root formation and auxin signaling?

Loss-of-function *PLC3* mutants displayed reduced lateral root densities (Fig. 1). This was due to less initiation sites, not development (data not shown). Promoter-GUS analyses revealed a typical, segmented, *PLC3*-expression pattern at the emerging site of the lateral root, whereby lateral roots always emerged from a segment but not every segment resulted in a lateral root. Normally, our agar plates are grown vertically in an angle of 80°, which typically gave two or three segments per lateral root. By tilting the agar plate more horizontally (45°), roots start to wiggle more and lateral root emerge at every bend (Ditengou et al. 2008). Using the latter setup drastically reduced the number of segments and revealed almost a 1:1 correlation between lateral roots emergence and *PLC3* expression. These results indicate that *PLC3* is required before lateral root initiation, and that at the 80° setup the primary root is less determined as to where and when it will produce a lateral root than the 45° setup where the decision is forced at the bending sites. That the phenotype in *plc3* mutants is quite mild may indicate redundancy of other *PLCs*. Using the eFP browser, we found three others, i.e. *PLC2*, *PLC5* and *PLC7* being also expressed in the phloem and/or companion cells (not shown; Winter et al. 2007).

Auxin plays an important role in lateral root formation and the mechanism by which auxin is perceived is well characterized (Péret et al. 2009a, 2009b; Benková and Bielach, 2010). The auxin receptor, TIR1 is an F-box protein in complex with SCF (ubiquitin protein ligase), which promotes ubiquitin-dependent proteolysis of the transcriptional repressor Aux/IAAs. Interestingly, IP_6 was found in the crystal structure of TIR1, where it is suggested to play a role in auxin binding and TIR1 function (Tan et al. 2007; Munnik, 2014). Where this IP_6 is coming from is unknown, but potentially this could be generated via PLC3 at the 'segments'. As such, less PLC3-generated IP_6 in the *plc3* mutants may explain the reduced auxin responsiveness (see Fig. 9A). That the effect is not so strong may well be due to redundant *PLCs*.

In seedlings, No difference in PPI- or PA levels between WT- and *plc3* seedlings were found (Supplemental Figs. S4 and S11A, B). Since PLC3 is only expressed in a limited number of cells (mainly phloem companion cells), it is possible that potential differences are in fact diluted-out in whole seedlings. We also did not observe major differences in the IPPs (Supplemental Figs. S10C-F), though slightly lower levels of IP_7 or IP_8 were found in *plc3* mutants, depending on seedling age and labeling procedure (Supplemental Figs. 11D, F). PP-IPPs are emerging as novel signaling molecules (Desai et al., 2014; Laha et al. 2015, 2016) for which there is already lots of evidence in yeast and animal cells (York, 2006; Michell, 2008; Burton et al. 2009; Shears, 2009). That PLC3 could be involved in generating such signaling molecules is exciting but requires further analysis. Similarly, other IPPs could be locally generated via this PLC. For example in guard cells, where IP_6 may be responsible for the release of intracellular Ca^{2+} (Lemtiri-Chlieh et al. 2000, 2003). For auxin, this type of Ca^{2+} signaling could also be relevant (Zhang et al. 2011). The main bottleneck still after the first discoveries >25 years ago (Gilroy et al. 1990; Blatt et al. 1990; Allen and Sanders, 1994), is the identification of a genuine IP_6- (or other IPP-) gated channel (Munnik 2014.

Several low phytic acid (LPA) mutants have been identified with reduced IP_6 levels in Arabidopsis. These include besides IPK1 and IPK2, inositol tris/tetrakisphosphate kinases (ITPKs), PI syntases (PISs) and AtMRP5 (Murphy et al. 2008; Nagy et al. 2009; Gonzalez et al. 2010; Kim and Tai, 2011; Desai et al. 2014; Kuo et al., 2014, 2017). The latter is not involved in IP_6 synthesis but in IP_6 transport, and shown to affect guard cell signaling, phytate storage and root architecture (Nagy et al. 2009.

Since RFOs are important for carbohydrate transport- and storage, they could be involved in loading sucrose to sink organs (Van den Ende, 2013; Sengupta et al. 2015; Gangl and Tenhaken, 2016), hence, affect lateral root density as sugars are stored in lateral roots. Since sugar transport occurs through the phloem where *PLC3* is specifically expressed, we analysed the sugar composition of the phloem sap of WT and *plc3* mutants. Interestingly, increased amounts of sucrose in the *plc3* mutants were found (Supplemental Fig. S9B). If sucrose is not properly transported to, or into, lateral roots via a tentative PLC-dependent RFO pathway, then sucrose levels could indeed be higher in the phloem, and theoretically affect root growth and lateral root formation. It will be worth to follow-up on this hypothesis using other *PLC* loss-of-fuction mutants that are also phloem expressed.

Role for *PLC3* in stomatal closure and ABA signaling

Both *plc3* mutants revealed reduced ABA responses, i.e. inhibition of seed germination and induction of stomatal closure (Figs. 3c and 4b). These results confirm earlier observations when PLC was silenced in tobacco (Hunt et al. 2003; Mills et al. 2004). We found that ABA triggered significant increases in PIP_2 in three different tissues, i.e. germinating seeds, guard-cell enriched leaf peels, and seedlings, and this response was reduced in *plc3* mutants or even lost in the germinating seeds and leaf peels, but not in the seedlings (Figs. 4, 6 and Supplemental Fig. S4). ABA may activate PLC3, causing an increase in PIP_2 hydrolysis, but also in its subsequent replenishment by PIP kinase (PIP5K). Due to

the nature of our ^{32}P-labeling experiments, synthesis of ^{32}P-PIP_2 may dominate the breakdown, hence be witnessed as an increase in PIP_2 (Munnik et al. 1998a, 1998b).

Earlier, PIP_2 has been implicated in stomatal opening (Lee et al. 2007). Exogenously administered PIP_2 induced swelling of guard-cell protoplasts and triggered stomatal opening. Moreover, a mutant of Arabidopsis PIP5K4 exhibited a reduced stomatal-opening phenotype, which could be rescued by complementation with the full-length *PIP5K4* or exogenous PIP_2 application (Lee et al. 2007). Electrophysiological experiments suggest that PIP_2 inhibits anion channel activity, likely SLAC1 (Lee et al. 2007), as well as K^+-efflux (Ma et al. 2009). A potential model summarising how PLC, PIP5K and PIP_2 could regulate stomatal opening is in Figure 9B. In the light, the H^+-ATPase pump is active, causing hyperpolarization of the plasma membrane and opening of the voltage-gated K^+-influx channel, KAT1. The subsequent influx of K^+ lowers the water potential and drives the net influx of water into the guard cell causing stomata to open. ABA-INSENSITIVE 1 (ABI1), a type 2C protein phosphatase (PP2C), inhibits SNF1-Related kinase 2 (SnRK2, i.e. OST1), preventing it from activating the slow anion channel 1 (SLAC1) (Munemasa et al. 2015; Assmann and Jegla, 2016). The PIP5K4-generated PIP_2 inhibits SLAC1 (Lee et al. 2007) and K^+-efflux (Ma et al. 2009), co-facilitating the low water potential. Upon ABA, the PYR/PYL-receptor dimer dissociates and forms PYR- or PYL-ABA complexes that bind PP2C so that I tcan then no longer inhibit SnRK2/OST1. As a consequence, SnRK2/OST1 auto-phosphorylates itself and activates SLAC1, which results in a decrease of intracellular Cl^- (Munemasa et al. 2015; Assmann and Jegla, 2016). In our model, ABA also activates PLC, which causes PIP_2 to be hydrolysed thereby releasing the inhibition of SLAC1 and K^+-efflux, and IPPs to be produced. IP_6 releases Ca^{2+} from internal stores (Lemtiri-Chlieh et al. 2000, 2003; Munnik, 2014), which in turn inhibits the K^+-influx channel (Lemtiri-Chlieh et al. 2000) and co-activates SLAC1 (Siegel et al. 2009). Together, these activities drive the net efflux of K^+ and Cl^-, causing water to leave the guard cells and stomatal pores to close. We propose that PLC3 is one of the PLCs involved in this process since the response is significantly reduced in *plc3* mutants. How PLC is activated by ABA remains elusive.

Overexpression of *PLC3* enhances drought tolerance

Plants use different strategies to cope with drought stress (Mickelbart et al. 2015; Zhu, 2016) and lipid signaling has been implicated as one of the factors in various plant systems (Munnik and Meijer, 2001; Meijer and Munnik, 2003; Munnik and Vermeer, 2010; Hou et al. 2016). Moreover, overexpression of a *PLC* in maize, tobacco and canola have been shown to improve drought tolerance (Wang et al. 2008; Georges et al. 2009; Tripathy et al. 2011). We showed here that overexpression of *PLC3* using the UBI10 promoter, improves drought tolerance in Arabidopsis. Under non-stressed conditions, *PLC3-OE* plants looked like WT but upon drought stress they clearly performed better (Figs. 7B, 7C). The molecular mechanism behind this may well reflect what is discussed above (Fig. 9B), but could also involve other factors, *e.g*. compatible solutes, gene expression, *etc*.

In an attempt to mimic drought in ^{32}P-prelabeled seedlings using sorbitol, increased PIP_2- and PA levels were found, and responses were stronger in the *PLC3-OE* lines (Fig. 8). Again, this may reflect the increased turnover of PIP_2 and phosphorylation of DAG that is readily picked-up by our method, although the increase in PA could also result from PLD activation (Munnik and Vermeer, 2010; Hou et al., 2016).

Since the UBQ10 promoter is constitutively expressed, the accumulation of PA and PIP_2 likely occurs in numerous cells and tissues, which is totally different from the local, endogenous *PLC3* expression in the vasculature and guard cells. Both lipids have been implicated as second messengers, playing roles in important cellular events, including regulation of the cytoskeleton, vesicular trafficking, and ion transport, and are likely to play a role in the plant's response to water stress (Munnik and Vermeer 2010; Testerink and Munnik, 2011; Ischenbeck and Heilmann, 2013; Heilmann, 2016, Gerth et al., 2017). Further unraveling of the molecular mechanisms involved requires identification and characterization of some main targets of these lipid second messengers. For PA this has already started (Testerink et al. 2004; McLoughlin et al. 2013; Testerink and McLoughlin, 2015), but for PIP_2 this is still an untouched area.

For many years, the PLC/IP_3/Ca^{2+} system has been claimed to regulate the gravitropism response (Perera et al. 1999; Stevenson et al. 2000; Perera et al. 2006; Boss et al. 2010). We tested this in our *plc3* mutants by rotating the agar plate by 90° and following their root growth direction (Supplemental Figs. S11A, B), but found no significant differences in bending between WT and *plc3* mutants (Supplemental Fig. S11C). This could be due to PLC redundancy. Most evidence for PLC/IP_3/Ca^{2+} enrollment in gravitropism is based on IP_3 measurements using an unreliable IP_3- displacement kit (Munnik, 2014). Since auxin is an important factor regulating gravitropism, an alternative hypothesis is that it reflects an IP_6-auxin link as described in Figure 9A (Zhang et al. 2011; Munnik 2014). Such hypothesis is equally interesting and deserves further investigation.

Materials and Methods

Plant material

Arabidopsis thaliana (Columbia-0, Col-0) T-DNA insertion mutants *plc3-2* (SALK_037453) and *plc3-3* (SALK_054406) were obtained from the SALK collection (signal.salk.edu). Homozygous plants were identified by PCR in the F2 generation using gene-specific primers in combination with left border primer, LBa (Supplemental Table 1).

RNA extraction and RT-PCR

Expression in the T-DNA insertion mutants was confirmed by RT-PCR. Total RNA was extracted with Trizol reagent (Invitrogen, Carlsbad, CA). RNA (5 μg) was converted to cDNA using oligo-dT18 primers, dNTPs and SuperScript III Reverse Transcriptase (Invitrogen) according to the manufacturer's

instructions. *PLC3* and *TUBLINα4* were PCR amplified for 40 or 30 cycles, respectively, with gene specific primers (Supplemental Table 1).

Cloning and plant transformation

To generate the reporter construct, $PLC3_{pro}$*::GUS-YFP*, a 2437-bp *PLC3* promoter region was amplified from genomic DNA using *PLC3prom HindIIIfw* 5'-CCCAAGCTTCAAGTCGCCGAACGAGACATC-3' and *PLC3prom NheIrev* 5' -CTGCTCTTCTTCTTCTTACTTGTTAG-3' and cloned into *HindIII/XbaI* digested *pJV-GUS-YFP*. The $PLC3_{pro}$*::GUS-YFP* cassette was transferred to pGreen0179 using *NotI.*

For the *PLC3* overexpressor, MultiSite Gateway Three-Fragment Vector Construction Kit (www.lifetechnologies.com) was used to generate $UBQ10_{pro}$*::PLC3* by cloning *PLC3* cDNA into pGreen0125 expression vector according to the supplier's protocol (www.thermofisher.com). Constructs were transformed into *Agrobacterium tumefaciens* strain GV3101, which was used to transform wild-type *Arabidopsis thaliana Col-0* by floral dip (Clough and Bent, 1998). Homozygous lines were selected in T3 generation and used for further experiments.

Real-time quantitative RT-PCR

The primer pairs used for conformation of *PLC3* (At4g38530) expression level were: 5'-TCCAGATTTCTTCGTCAAGATTGGA-3' (forward) and 5'-TATAGGAAACCACTGATCGACAGC-3' (reverse). For cDNA synthesis, 1 μg of total RNA from 10-day-old seedlings was used. Q-PCR analyses was performed with an ABI 7500 Real-Time PCR System (Applied Biosystem). The relative gene expression was determined by comparative threshold cycle value. Transcript levels were normalized by the level of *SAND* (At2g28390; forward primer: 5'-AAC TCT ATG CAG CAT TTG ATC CAC T-3', reverse primer: 5'-TGA TTG CAT ATC TTT ATC GCC ATC-3') (Han et al. 2013). Three biological replicates and two technical replicates were used to calculate means and standard deviations.

Histochemical analyses for GUS activity

GUS staining was performed according to the method described by Jefferson et al. (1987) with minor modifications. Transgenic plants carrying $PLC3_{pro}$*:GUS-YFP* were grown for indicated times and specific tissues were taken and incubated in X-Gluc reaction solution containing 1 mg/ml 5-bromo-4-chloro-3 indolyl-β-D-glucuronic acid (X-gluc) in 50 mM phosphate buffer (pH 7.0) and 0.1% TX-100. Materials were incubated overnight at 37°C. Next day, the solution was replaced by 70% ethanol to destain the tissue. Plant tissues were viewed under a stereo microscope (Leica MZFLIII) and photographed (ThorLabs CCD camera). Three independent lines were tested showing the same results.

Confocal microscopy

Arabidopsis *PLC3$_{pro}$:GUS-YFP* seedlings were grown for 5 days and then transferred to object slides containing a fixed cover slide that was separated by a spacer of approximately 0.32 mm (Munnik and Zarza, 2013). This allowed seedlings to grow in liquid medium (½ Murashi-Skoog (½MS) with 1% sucrose, pH 5.8) for 1-2 days so that they could directly be used for microscopy without damage to the root hairs. Microscopy was performed using a Zeiss LSM 510 CLSM (confocal laser scanning microscope) (Carl-Zeiss GMBH, Jena, Germany), implemented on an inverted microscope (Axiovert 100, Carl-Zeiss GMBH, Jena, Germany). For YFP imaging, confocal configurations were used as described before (Vermeer et al. 2006).

Seed germination

Mature seeds were harvested and stored at room temperature. Seeds were surface sterilized with chlorine gas in a desiccator by using 20 ml bleach (5% NaClO) and 1 ml 37% HCl for 3 h, then sown on square petri dishes containing 30 ml ½MS medium, 0.5% sucrose, pH 5.8, and 1.2 % Daishin agar ± ABA (0, 1, 2 μM), and kept in the dark for two days at 4 °C, afterwhich the plates were transferred to long-day conditions (i.e. 22 °C, 16 h of light and 8h of dark). Germination was scored as radical emergence at indicated time points using a binocular microscope (Leica MZFLIII).

Root growth

Seeds were sterilized and stratified as described above. Plates were transfered to long-day conditions and placed vertically under an angle of 80°. Four-day-old seedlings with comparable size were then transfered to ½MS ager plate. Plates were imaged 8 days later (12 DAG) using an Epson Perfection V700 scanner. Primary root length and lateral root number for each genotype was quantified by ImageJ analysis software (National Institute of Health (NIH)). Lateral root density was expressed as the lateral number per primary root length (LR number/ PR length). For gravitropic responses, seedlings were grown on ½MS plates with 0.5% sucrose for four days. Plates were then rotated 90° and scanned two days later. Bending was expressed as curvature angle, which was quantified by ImageJ analysis software (NIH) (Perera et al. 2006).

Stomatal aperture

Stomatal apertures were measured according to Distéfano et al. (2012) with some minor changes. Treatments were performed on epidermal leaf strips excised from the abaxial side of fully expanded Arabidopsis leaves from 3-week-old plants grown at 22°C for 16 h of light and 8h of dark. Strips were floated onto 'opening buffer' containing 5 mM MES-KOH, pH 6.1 and 50 mM KCl for 3 h. Strips were maintained in the same opening buffer and exposed to different ABA concentrations. After 90 min, stomata were digitized using a Nikon DS-Fi 1 camera, coupled to a Nikon Eclipse Ti microscope. The stomatal-aperture width was measured using ImageJ (NIH).

$^{32}P_i$-phospholipid labeling, extraction and analysis

For the determination of PPI- and PA levels, different tissues were $^{32}P_i$-labeled, including germinating seeds, leaf peels, and seedlings:

Germinating seeds: Seeds were sterilized and stratified on ½MS with 0.5% sucrose (pH 5.8) and germinated under long day condition for around 20 h when testa ruptured. Germinating seeds were then transferred to 200 µl labeling buffer (2.5 mM MES, pH 5.8, 1 mM KCl) containing 5-10 µCi $^{32}PO_4^{3-}$ ($^{32}P_i$) (carrier free; Perklin-Elmer) in 2 ml Eppendorf Safelock microcentrifuge tubes for 24 h. Samples were treated with 200 µl buffer ± ABA for the times and concentrations indicated.

Epidermal leaf peels: Leaves of 3-week-old plants grown at 22°C under 16 h of light and 8 h of dark were stripped and immediately floated on 100 µl opening buffer (10 mM MES, pH 6.1 and 50 mM KCl) containing $^{32}P_i$ (5-10 µCi) in a 48-wells cell culture plate (Greiner bio-one) for 3 h. Samples were treated with 400 µl buffer (10 mM MES-KOH, pH 6.1, 2.5 µM $CaCl_2$) supplemented with or without ABA for the times and concentrations indicated.

Seedlings: Five-day-old seedlings were transferred to 200 µl labeling buffer (2.5 mM MES-KOH, pH 5.8, 1 mM KCl) containing $^{32}P_i$ (5-10 µCi) in 2 ml Eppendorf tubes and labeled overnight (~16 h) or 3h. Samples were treated the next day by adding 200 µl labeling buffer, supplemented with or without ABA or sorbitol for the times and concentrations indicated.

All treatments were stopped by adding perchloric acid to a final concentration of 5% (v/v) for 5-10 min, after which the supernatant was removed (2' 13.000 g) and the lipids extracted with 400 µl of $CHCl_3$/MeOH/HCl [50:100:1 v/v)]. After 15 min, 400 µl of $CHCl_3$ was added, followed by 200 µl of 0.9 % (w/v) NaCl to separate the extract into two phases. The organic lipid fraction was washed and concentrated as described earlier (Munnik & Zarza, 2013). Lipids were separated by thin-layer chromatography (TLC) using an alkaline solvent system, containing: chloroform/methanol/25% ammonia/water [90:70:4:16 (v/v)] (Munnik et al. 1994a,b). Radioactive phospholipids were visualized by autoradiography and quantified by phosphoimaging (Typhoon FLA 7000, GE Healthcare). Individual phospholipid levels were expressed as the percentage of the total ^{32}P-lipid fraction.

Inositolpolyphosphates – [^{3}H-Ins] labeling, extraction and HPLC Analyses

For the measurement of inositolpolyphosphates (IPPs), two labeling procedures were used. The first was based on the method described by Laha et al. (2015). Seedlings were grown under short day (22 °C, 12 h light/12h dark) in ½MS containing 2% sucrose, pH 5.7, and 0.6% phytagel for 11 days, after which 10 seedlings were transferred to 2 ml liquid medium (¼MS, pH 5.7, 0.3 % phytagel) containing ^{3}H-*myo*-inositol (80 µCi; Biotrend, ART-0261-5, Cologne, Germany). After 7 days, seedlings were washed twice with water before harvesting and snap-freezed into liquid N_2. IPPs were subsequently extracted (Azevedo and Saiardi, 2006) and resolved by strong anion exchange chromatography HPLC (using the Partisphere SAX 4.6 x 125mm column; Whatman) at a flow rate of 0.5 mL/min, using a shallow gradient formed by buffer A (1 mM EDTA) and buffer B (1.3 M ammonium phosphate (pH 3.8, H_3PO_4), 1 mM EDTA). Fractions were collected every minute and radioactivity quantified by liquid

scintillation counting. Results are expressed as percentage of total. The latter was determined by counting ^{3}H in all fractions from 13 min to the end of the run.

Alternatively, IPPs were determined as described by Desai et al. (2014). In this case, seedlings were grown in ½MS with 0.8 % agar under long-day conditions (16 h day and 8 h dark) for 4 days, afterwhich 15 seedlings were incubated in 50 µl medium (1x MS, 1% sucrose, pH 5.7) supplemented with 100 µl of aqueous *Myo* [2-^{3}H(N)]-inositol (100 µCi; American Radiolabeled Chemicals Cat. #ART 0116A; specific activity 20 Ci/mmol). Samples were incubated with supplemental light for 4 days. IPPs were extracted as described by Azevedo and Saiardi (2006), by vortexing the tissue with glass beads in extraction buffer (25 mM EDTA, 10 mg/ml IP_6 and 1M $HClO_4$). Samples were neutralized to ~pH 6 to 8 with 250 mM EDTA, 1M K_2CO_3 and dried to a volume of 70 µl. Samples were separated using a binary HPLC pump (Beckman Coulter) equipped with a Partisphere-SAX (4.6 x 125 mm) column and guard cartridge. The elution gradient was set up as described by Azevedo and Saiardi (2006) using the same buffers as above, at a flow rate of 1 ml/min. An on-line IN/US radiation detector was used to generate chromatograms. Four ml of Ultima-Flo AP scintillation cocktail (Perkin Elmer, Waltham, MA, USA) was added to each 1 ml eluted fraction post-detector to quantify the radioactivity of the eluted fractions using the ^{3}H window of a Beckman Coulter LS6500 Scintillation Counter. The ^{3}H-*myo*-Ins cpm incorporated into total IPPs was calculated by taking the sum of cpm of all fractions and subtracting the peak of free ^{3}H-Ins cpm. The amount of each IPP was calculated as follows: [(Σ cpms in peak) / (total IPP)]*100].

Drought tolerance

Determination of survival rates, fresh weight (FW) and dry weight (DW) under water deficit condition and water loss were performed as described in the literature (Hua et al. 2012; Osakabe et al. 2013), with some minor modifications. Seeds were stratified in the dark for 2 nights at 4°C and directly sown on soil (pots 4.5 cm x 4.5 cm x 7.5 cm), with each pot containing nine plants and 80 g of soil. Plants were grown at short day conditions (22 °C with 12 h light/12 h dark) for 4 weeks and then subjected to drought stress by withholding them for water for 2 weeks, while control plants were normally watered. Plants were photographed, re-watered for another week and again photographed. Surviving green plants were counted and the survival rate determined by the percentage of green plants compared to total amount of plants. Each experiment used 36 plants per genotype and experiments were repeated at least 3 times.

To determine the FW and DW under dehydration stress, plants were grown under short day conditions for four weeks as described above, and exposed to drought for 1 week by water withholding, while control plants were normally watered. Rosette FWs were scored immediately after detachment by weighing. After complete drying, DWs were determined. Eighteen plants from each genotype were measured and the experiment was repeated 3 times.

To assay water-loss, rosettes from 4-week-old plants were detached and the FW determined every hour by weighing on a scale. Water content was calculated as a percentage of the initial FW. Twenty plants were used for each experiment and the experiment was repeated at least 3 times.

Funding

This work was supported by the China Scholarship Council [201206300058 to Q.Z.]; the Pakistan Higher Education Commission [2-3(70)/PDFP/HEC/2008/2 to MS]; the Netherlands Organization for Scientific Research [813.06.003, 864.05.001, and 867.15.020 to T.M.], and the Deutsche Forschungsgemeinschaft (SFB 1101/TP A05 and research grant SCHA 1274/4-1 to G.S.).

Disclosures

No conflicts of interest declared

Acknowledgements

We thank Max van Hooren for critically reading the manuscript.

References

Abd-El-Haliem, A.M., and Joosten, M.H. (2017) Plant phosphatidylinositol-specific phospholipase C at the center of plant innate immunity. *J Integr Plant Biol*. **59**, 164-179.

Abd-El-Haliem, A., Meijer, H.J., Tameling, W.I., Vossen, J.H., Joosten, M.H. (2012) Defense activation triggers differential expression of phospholipase-C (*PLC*) genes and elevated temperature induces phosphatidic acid (PA) accumulation in tomato. *Plant Signal Behav*. **7**, 1073-1078.

Allen, G.J., & Sanders, D. (1994). Osmotic stress enhances the competence of *Beta vulgaris* vacuoles to respond to inositol 1,4,5-trisphosphate. *Plant J.* **6**, 687-695.

Arisz SA & Munnik T. (2013) Distinguishing phosphatidic acid pools from *de novo* synthesis, PLD and DGK. *Methods Mol. Biol*. **1009**, 55-62.

Arisz, S.A., van Wijk, R., Roels, W., Zhu, J-K., Haring, M. A., & Munnik, T. (2013). Rapid phosphatidic acid accumulation in response to low temperature stress in Arabidopsis is generated through diacylglycerol kinase. *Front Plant Sci.* **4**, 1-15.

Arisz, S.A, Testerink, C., & Munnik, T. (2009). Plant PA signaling via diacylglycerol kinase. *Biochim. Biophys. Acta* **1791**, 869-75.

Assmann, S.M., & Jegla, T. (2016). Guard cell sensory systems: recent insights on stomatal responses to light, abscisic acid, and CO2. *Curr. Opin. Plant Biol.* **33**, 157-167.

Balla, T. (2013). Phosphoinositides: tiny lipids with giant impact on cell regulation. *Physiol. Rev.* **93**, 1019-1137.

Benková, E., & Bielach, A. (2010). Lateral root organogenesis - from cell to organ. *Curr. Opin. Plant Biol.* **13**, 677-83.

Blatt, M.R. (2000). Cellular signaling and volume control in stomatal movements in plants. *Annu. Rev. Cell Dev. Biol.* **16**, 221-41.

Blatt, M.R., Thiel, G., & Trentham, D.R. (1990). Reversible inactivation of K^+ channels of Vicia stomatal guard cells following the photolysis of caged inositol 1,4,5-trisphosphate. *Nature* **346**, 766-769.

Boss, W.F., Sederoff, H.W., Im, Y.J., Moran, N., Grunden, A.M., & Perera, I.Y. (2010). Basal signaling regulates plant growth and development. *Plant Physiol.* **154**, 439-443.

Burton, A., Hu, X., & Saiardi, A. (2009). Are inositol pyrophosphates signaling molecules? *J. Cell. Physiol.* **220**, 8-15.

Cho, M.H., Shears, S.B., & Boss, W.F. (1993). Changes in phosphatidylinositol metabolism in response to hyperosmotic stress in *Daucus carota* L. cells grown in suspension culture. *Plant Physiol.* **103**, 637-647.

Clough, S.J., & Bent, A.F. (1998). Floral dip: A simplified method for Agrobacterium-mediated transformation of *Arabidopsis thaliana*. *Plant J.* **16**, 735-743.

D'Ambrosio, J.M., Couto, D., Fabro, G., Scuffi, D., Álvarez, M.E., Lamattina, L., Munnik, T., Andersson, M.X., Zipfel, C., Laxalt, A.M. (2017) PLC2 regulates MAMP-triggered immunity by modulating ROS production in Arabidopsis. *Plant Phys.* Accepted.

Darwish, E., Testerink, C., Khalil, M., El-Shihy, O., & Munnik, T. (2009). Phospholipid signaling responses in salt-stressed rice leaves. *Plant Cell Physiol.* **50**, 986-97.

Das, S., Hussain, A., Bock, C., Keller, W.A., & Georges, F. (2005). Cloning of *Brassica napus* phospholipase C2 (*BnPLC2*), phosphatidylinositol 3-kinase (*BnVPS34*) and phosphatidylinositol synthase1 (*BnPtdIns S1*) - Comparative analysis of the effect of abiotic stresses on the expression of phosphatidylinositol signal transduction-related genes in *B. napus*. *Planta* **220**, 777-784.

De Jong, C.F., Laxalt, A.M., Bargmann, B.O.R., De Wit, P.J.G.M., Joosten, M.H.A.J., & Munnik, T. (2004). Phosphatidic acid accumulation is an early response in the Cf-4/Avr4 interaction. *Plant J.* **39**, 1-12.

Desai, M., Rangarajan, P., Donahue, J.L., Williams, S.P., Land, E.S., Mandal, M.K., *et al.* (2014). Two inositol hexakisphosphate kinases drive inositol pyrophosphate synthesis in plants. *Plant J.* **80**, 642-653.

DeWald, D.B., Torabinejad, J., Jones, C.A., Shope, J.C., Cangelosi, A.R., Thompson, J.E., *et al*. (2001). Rapid accumulation of phosphatidylinositol 4,5-bisphosphate and inositol 1,4,5-trisphosphate correlates with calcium mobilization in salt-stressed Arabidopsis. *Plant Physiol.*, **126**, 759-769.

Di Fino, L., D'Ambrosio, J., Tejos, R., van Wijk, R., Lamattina, T., Munnik, T., *et al.* (2017). Arabidopsis phosphatidylinositol-phospholipase C2 (*PLC2*) is involved in female gametogenesis and embryo development. *Planta* **245**, 717-728.

Distéfano, A.M., Scuffi, D., García-Mata, C., Lamattina, L., & Laxalt, A.M. (2012). Phospholipase Dδ is involved in nitric oxide-induced stomatal closure. *Planta* **236**, 1899-1907.

Ditengou, F.A., Teale, W.D., Kochersperger, P., Flittner, K.A., Kneuper, I., van der Graaff, E., *et al.* (2008). Mechanical induction of lateral root initiation in *Arabidopsis thaliana*. *Proc. Natl. Acad. Sci. USA* **105**, 18818-18823.

Dowd, P.E., Coursol, S., Skirpan, A.L., Kao, T., & Gilroy, S. (2006). Petunia phospholipase C1 is involved in pollen tube growth. *Plant Cell* **18**, 1438-1453.

Flores, S., & Smart, C.C. (2000). Abscisic acid-induced changes in inositol metabolism in *Spirodela polyrrhiza*. *Planta* **211**, 823-832.

Gaedeke N., Klein M., Kolukisaoglu U., Forestier C., Müller A., Ansorge M., *et al.* (2001) The *Arabidopsis thaliana* ABC transporter AtMRP5 controls root development and stomata movement. *EMBO J.* **20**, 1875-1887.

Gangl, R., & Tenhaken, R. (2016). Raffinose family oligosaccharides act as galactose stores in seeds and are required for rapid germination of Arabidopsis in the dark. *Front. Plant Sci.* **7**, 1-15.

Gao, K., Liu, Y.L., Li, B., Zhou, R.G., Sun, D.Y., & Zheng, S.Z. (2014). *Arabidopsis thaliana* phosphoinositide-specific phospholipase C isoform 3 (*AtPLC3*) and *AtPLC9* have an additive effect on thermotolerance. *Plant Cell Physiol.* **55**, 1873-1883.

Georges, F., Das, S., Ray, H., Bock, C., Nokhrina, K., Kolla, V.A., *et al.* (2009). Over-expression of *Brassica napus* phosphatidylinositol-phospholipase C2 in canola induces significant changes in gene expression and phytohormone distribution patterns, enhances drought tolerance and promotes early flowering and maturation. *Plant Cell Environ.* **32**, 1664-1681.

Gerth, K., Lin, F., Menzel, W., Krishnamoorthy, P., Stenzel, I., Heilmann, M., Heilmann, I. (2017) Guilt by association: A phenotype-based view of the plant phosphoinositide network. *Annu Rev Plant Biol.* **68**, 349-374

Gillaspy, G.E. (2011). The cellular language of myo-inositol signaling. *New Phytol.* **192**, 823-839.

Gillaspy, G.E. (2013). The role of phosphoinositides and inositol phosphates in plant cell signaling. *Adv Exp Med Biol.* **991**, 141-157.

Gilroy, S., Read, N.D., & Trewavas, A.J. (1990). Elevation of cytoplasmic calcium by caged calcium or caged inositol triphosphate initiates stomatal closure. *Nature* **346**, 769-771.

Gonorazky, G., Guzzo, M. C., & Laxalt, A.M. (2016). Silencing of the tomato phosphatidylinositol-phospholipase C2 (SlPLC2) reduces plant susceptibility to *Botrytis cinerea*. *Molecular Plant Pathology* **2**, 1-10.

Gonorazky, G., Ramirez, L., Abd-El-Haliem, A., Vossen, J.H., Lamattina, L., ten Have, A., *et al.* (2014). The tomato phosphatidylinositol-phospholipase C2 (SlPLC2) is required for defense gene induction by the fungal elicitor xylanase. *J. Plant Physiol.* ***171***, 959-965.

Gonzalez, B., Banos-Sanz, J.I., Villate, M., Brearley, C.A., and Sanz-Aparicio, J. (2010). Inositol 1,3,4,5,6-pentakisphosphate 2-kinase is a distant IPK member with a singular inositide binding site for axial 2-OH recognition. *Proc. Natl. Acad. Sci. USA* **107,** 9608-9613.

Guelette, B.S., Benning, U.F., & Hoffmann-Benning, S. (2012) Identification of lipids and lipid-binding proteins in phloem exudates from *Arabidopsis thaliana*. *J. Exp. Bot.* **63**, 3603-3616.

Han, B., Yang, Z., Samma, M.K., Wang, R., & Shen, W. (2013). Systematic validation of candidate reference genes for qRT-PCR normalization under iron deficiency in Arabidopsis. *BioMetals* **26**, 403-413.

Hartog, M. Den, Verhoef, N., & Munnik, T. (2003). Nod factor and elicitors activate different phospholipid signaling pathways in suspension-cultured Alfalfa cells. *Plant Physiol.* **132**, 311-317.

Heilmann, I. (2016). Phosphoinositide signaling in plant development. *Development* **143**, 2044-2055.

Heilmann, I. and Ischebeck, T. (2016) Male functions and malfunctions: the impact of phosphoinositides on pollen development and pollen tube growth. *Plant Reprod.* **29**, 3-20.

Helling, D., Possart, A., Cottier, S., Klahre, U., & Kost, B. (2006). Pollen tube tip growth depends on plasma membrane polarization mediated by tobacco PLC3 activity and endocytic membrane recycling. *Plant Cell* **18**, 3519-3534.

Hirayama, T., Ohtot, C., Mizoguchi, T., & Shinozaki, K. (1995). A gene encoding a phosphatidylinositol-specific phospholipase C is induced by dehydration and salt stress in *Arabidopsis thaliana. Proc. Natl. Acad. Sci. USA* **92**, 3903-3907.

Hirayama, T., & Umezawa, T. (2010). The PP2C-SnRK2 complex. *Plant Signal. & Behav.* **5**, 160-163.

Horvath, I., Glatz, A., Nakamoto, H., Mishkind, M. L., Munnik, T., Saidi, Y., *et al.* (2012). Heat shock response in photosynthetic organisms: Membrane and lipid connections. *Prog. Lipid Res* **51**, 208-220.

Hou, Q., Ufer, G., & Bartels, D. (2016). Lipid signaling in plant responses to abiotic stress. *Plant Cell Environ.* **39**, 1029-1048.

Hua, D., Wang, C., He, J., Liao, H., Duan, Y., Zhu, Z., *et al.* (2012). A plasma membrane receptor kinase, GHR1, mediates abscisic acid- and hydrogen peroxide-regulated stomatal movement in Arabidopsis. *Plant Cell* **24**, 2546-61.

Hunt, L., & Gray, J.E. (2001). ABA signaling: A messenger's FIERY fate. *Curr. Biol.* **11**, 968-970.

Hunt, L., Mills, L.N., Pical, C., Leckie, C.P., Aitken, F.L., Kopka, J., *et al.* (2003). Phospholipase C is required for the control of stomatal aperture by ABA. *Plant J.* **34**, 47-55.

Hunt, L., Otterhag, L., Lee, J.C., Lasheen, T., Hunt, J., Seki, M., *et al.* (2004). Gene-specific expression and calcium activation of *Arabidopsis thaliana* phospholipase C isoforms. *New Phytol.* **162**, 643-654.

Ischebeck, T.Seiler, S. and Heilmann, I., (2010) At the poles across kingdoms: phosphoinositides and polar tip growth. *Protoplasma*. **240**, 13-31.

Irvine, R. F. (2006). Nuclear inositide signaling – Expansion, structures and clarification. *Biochim Biophys Acta.* **1761**, 505-508.

Jefferson, R.A., Kavanagh, T. A., & Bevan, M.W. (1987). GUS fusions: beta-glucuronidase as a sensitive and versatile gene fusion marker in higher plants. *EMBO J.* **6**, 3901-3907.

Kim, S.I., and Tai, T.H. (2011). Identification of genes necessary for wild-type levels of seed phytic acid in *Arabidopsis thaliana* using a reverse genetics approach. *Mol. Genet. Genomics* **286,** 119-133.

Kuo, H.F., Chang, T.Y., Chiang, S.F., Wang, W.D., Charng, Y.Y., and Chiou, T.J. (2014). Arabidopsis inositol pentakisphosphate 2-kinase, AtIPK1, is required for growth and modulates phosphate homeostasis at the transcriptional level. *Plant J.* **80,** 503-515.

Laha, D., Johnen, P., Azevedo, C., Dynowski, M., Weiß, M., Capolicchio, S., *et al.* (2015). VIH2 regulates the synthesis of inositol pyrophosphate $InsP_8$ and jasmonate-dependent defenses in Arabidopsis. *Plant Cell* **27**, 1082-1097.

Laha, D., Parvin, N., Dynowski, M., Johnen, P., Mao, H., Bitters, S. T., *et al.* (2016). Inositol polyphosphate binding specificity of the jasmonate receptor complex. *Plant Physiol.* **171**, 2364-2370.

Lanteri, M.L., Lamattina, L., & Laxalt, A.M. (2011). Mechanisms of xylanase-induced nitric oxide and phosphatidic acid production in tomato cells. *Planta* **234**, 845-855.

Laxalt, A. M., & Munnik, T. (2002). Phospholipid signaling in plant defence. *Curr. Opin. Plant Biol.* **5**, 332-338.

Lee, Y., Choi, Y.B., Suh, S., Lee, J., Assmann, S.M., Joe, C. O., *et al.* (1996). Abscisic acid-induced phosphoinositide turnover in guard cell protoplasts of *Vicia faba*. *Plant Physiol* **110**, 987-996.

Lee, Y., Kim, Y.W., Jeon, B.W., Park, K. Y., Suh, S.J., Seo, J., *et al.* (2007). Phosphatidylinositol 4,5-bisphosphate is important for stomatal opening. *Plant J.* **52**, 803-816.

Lemtiri-Chlieh, F., MacRobbie, E.A.C., & Brearley, C.A. (2000). Inositol hexakisphosphate is a physiological signal regulating the K^+-inward rectifying conductance in guard cells. *Proc. Natl. Acad. Sci. USA* **97**, 8687-8692.

Lemtiri-Chlieh, F., MacRobbie, E.AC., Webb, A.AR., Manison, N.F., Brownlee, C., Skepper, J.N., *et al.* (2003). Inositol hexakisphosphate mobilizes an endomembrane store of calcium in guard cells. *Proc. Natl. Acad. Sci. USA* **100**, 10091-10095.

Li, L., He, Y., Wang, Y., Zhao, S., Chen, X., Ye, T., *et al.* (2015). Arabidopsis PLC2 is involved in auxin-modulated reproductive development. *Plant J.* **84**, 504-515.

Liu, H.T., Huang, W. D., Pan, Q. H., Weng, F. H., Zhan, J.C., Liu, Y., *et al.* (2006a). Contributions of PIP_2-specific-phospholipase C and free salicylic acid to heat acclimation-induced thermotolerance in pea leaves. *J. Plant Physiol.* **163**, 405-416.

Liu, H.T., Liu, Y.Y., Pan, Q. H., Yang, H.R., Zhan, J.C., & Huang, W.D. (2006b). Novel interrelationship between salicylic acid, abscisic acid, and PIP_2-specific phospholipase C in heat acclimation-induced thermotolerance in pea leaves. *J. Exp. Bot.* ***57***, 3337-3347.

Luit, A.H. van der, Piatti, T., Doorn, A. Van, Musgrave, A., Felix, G., Boller, T., & Munnik, T. (2000). Elicitation of suspension-cultured tomato cells triggers the formation of phosphatidic acid and diacylglycerol pyrophosphate. *Plant Physiol.* **123**, 1507-1515.

Luo, Y., Xie, W., & Luo, F. (2012). Effect of several germination treatments on phosphatases activities and degradation of phytate in Faba Bean (*Vicia faba* L.) and Azuki Bean (*Vigna angularis* L.). *J Food Sci.* **77** 1023-1029.

Meijer, H. J. G., & Munnik, T. (2003). Phospholipid-based signaling in plants. *Annu. Rev. Plant Biol.* **54**, 265-306.

Michell, R.H. (2008). Inositol derivatives: evolution and functions. *Nature Rev.* **9**, 151-161.

Mickelbart, M.V., Hasegawa, P.M., & Bailey-Serres, J. (2015). Genetic mechanisms of abiotic stress tolerance that translate to crop yield stability. *Nature Rev. Gen.* **16**, 237-251.

Mills, L.N., Hunt, L., Leckie, C.P., Aitken, F.L., Wentworth, M., McAinsh, M.R., … Hetherington, A.M. (2004). The effects of manipulating phospholipase C on guard cell ABA-signaling. *J. Exp. Bot.* **55**, 199-204.

Mishkind, M., Vermeer, J.E.M., Darwish, E., & Munnik, T. (2009). Heat stress activates phospholipase D and triggers PIP_2 accumulation at the plasma membrane and nucleus. *Plant J.* **60**, 10-21.

Munemasa, S., Hauser, F., Park, J., Waadt, R., Brandt, B., & Schroeder, J.I. (2015). Mechanisms of abscisic acid-mediated control of stomatal aperture. *Curr. Opin. Plant Biol.* **28**, 154-162.

Munnik, T. (2001). Phosphatidic acid: an emerging plant lipid second messenger. *Trends Plant Sci.* **6**, 227-233.

Munnik, T. (2014). PI-PLC: Phosphoinositide-phospholipase C in plant signaling. *In* Phospholipases in Plant Signaling. Wang X. (Ed.), Signaling and Communication in Plants **20**, Springer-Verlag, Berlin Heidelberg. pp 27-54.

Munnik, T., Irvine, R.F., Musgrave, A. (1998a) Phospholipid signalling in plants. *Biochim. Biophys. Acta*, **1389**: 222-272.

Munnik, T. & Laxalt, A.M. (2013) Measuring PLD activity *in vivo*. *Methods Mol. Biol.* **1009**, 219-232.

Munnik, T., & Meijer, H. J. G. (2001). Osmotic stress activates distinct lipid and MAPK signaling pathways in plants. *FEBS Letters* **498**, 172-178.

Munnik, T., Musgrave, A., & de Vrije, T. (1994). Rapid turnover of polyphosphoinositides in carnation flower petals. *Planta*, *193*, 89-98.

Munnik, T., & Nielsen, E. (2011). Green light for polyphosphoinositide signals in plants. *Current Opinion in Plant Biology*, **14**, 489-97.

Munnik, T., & Testerink, C. (2009). Plant phospholipid signaling: "in a nutshell". *J Lipid Res.* **50**, S260-S265.

Munnik, T., van Himbergen, J.A.J., ter Riet, B., Braun, F.-J., Irvine, R.F., van den Ende, H., *et al.* (1998b). Detailed analysis of the turnover of polyphosphoinositides and phosphatidic acid upon activation of phospholipases C and D in *Chlamydomonas* cells treated with non-permeabilizing concentrations of mastoparan. *Planta* **207**, 133-145.

Munnik, T., & Vermeer, J.E.M. (2010). Osmotic stress-induced phosphoinositide and inositol phosphate signaling in plants. *Plant, Cell & Environment* **33**, 655-669.

Munnik, T. & Zarza, X. (2013) Analyzing plant signaling phospholipids through $^{32}P_i$-labeling and TLC. *Methods Mol. Biol.* **1009**, 3-15.

Murphy, A.M., Otto, B., Brearley, C.A., Carr, J.P., and Hanke, D.E. (2008). A role for inositol hexakisphosphate in the maintenance of basal resistance to plant pathogens. *Plant J.* **56,** 638-652.

Nagy, R., Grob, H., Weder, B., Green, P., Klein, M., Frelet-Barrand, A., *et al.* (2009). The Arabidopsis ATP-binding cassette protein AtMRP5/AtABCC5 is a high affinity inositol hexakisphosphate transporter involved in guard cell signaling and phytate storage. *J. Biol. Chem.* **284,** 33614-33622.

Nakashima, K., & Yamaguchi-Shinozaki, K. (2013). ABA signaling in stress-response and seed development. *Plant Cell Reports* **32**, 959-970.

Nambara, E., Okamoto, M., Tatematsu, K., Yano, R., Seo, M., & Kamiya, Y. (2010). Abscisic acid and the control of seed dormancy and germination. *Seed Science Res.* **20**, 55-67.

Nokhrina, K., Ray, H., Bock, C., & Georges, F. (2014). Metabolomic shifts in *Brassica napus* lines with enhanced *BnPLC2* expression impact their response to low temperature stress and plant pathogens. *GM Crops & Food* **5**, 120-131.

Otegui, M.S., Capp, R., & Staehelin, L.A. (2002). Developing seeds of Arabidopsis store different minerals in two types of vacuoles and in the endoplasmic reticulum. *Plant Cell* **14**, 1311-1327.

Perera, I.Y., Heilmann, I., & Boss, W.F. (1999). Transient and sustained increases in inositol 1,4,5-trisphosphate precede the differential growth response in gravistimulated maize pulvini. *Proc. Natl. Acad. Sci. USA* **96**, 5838-5843.

Perera, I.Y., Hung, C., Brady, S., Muday, G.K., & Boss, W.F. (2006). A universal role for inositol 1,4,5-trisphosphate-mediated signaling in plant gravitropism. *Plant Physiol.* **140**, 746-760.

Péret, B., De Rybel, B., Casimiro, I., Benková, E., Swarup, R., Laplaze, L., *et al.* (2009). Arabidopsis lateral root development: an emerging story. *Trends Plant Sci.* 14, 399-408.

Péret, B., Larrieu, A., & Bennett, M.J. (2009). Lateral root emergence: A difficult birth. *J. Exp. Botany* **60**, 3637-3643.

Pical, C., Westergren, T., Dove, S. K., Larsson, C., & Sommarin, M. (1999). Salinity and hyperosmotic stress induce rapid increases in phosphatidylinositol 4,5-bisphosphate, diacylglycerol pyrophosphate, and phosphatidylcholine in *Arabidopsis thaliana* cells. *J. Biol. Chem.* **274**, 38232-38240.

Pokotylo, I., Kolesnikov, Y., Kravets, V., Zachowski, A., & Ruelland, E. (2014). Plant phosphoinositide-dependent phospholipases C: Variations around a canonical theme. *Biochimie* **96**, 144-157.

Raho, N., Ramirez, L., Lanteri, M.L., Gonorazky, G., Lamattina, L., ten Have, A., *et al*. Phosphatidic acid production in chitosan-elicited tomato cells, via both phospholipase D and phospholipase C/diacylglycerol kinase, requires nitric oxide. *J. Plant Physiol.* **168**, 534-539.

Repp, A., Mikami, K., Mittmann, F., & Hartmann, E. (2004). Phosphoinositide-specific phospholipase C is involved in cytokinin and gravity responses in the moss *Physcomitrella patens*. *Plant J.* **40**, 250-259.

Ribeiro, P.R., Fernandez, L. G., de Castro, R.D., Ligterink, W., & Hilhorst, H.W. (2014). Physiological and biochemical responses of Ricinus communis seedlings to different temperatures: a metabolomics approach. *BMC Plant Biology* **14**, 1-14.

Rodriguez-Villalon, A., Gujas, B., van Wijk, R., Munnik, T., & Hardtke, C.S. (2015). Primary root protophloem differentiation requires balanced phosphatidylinositol-4,5-bisphosphate levels and systemically affects root branching. *Development* **142**, 1437-1446.

Roessner, U., Wagner, C., Kopka, J., Trethewey, R.N. & Willmitzer, L. 2000. Simultaneous analysis of metabolites in potato tuber by gas chromatography-mass spectrometry. *Plant J.* **23**, 131-142.

Ruelland, E., Cantrel, C., Gawer, M., Kader, J.C., & Zachowski, A. (2002). Activation of phospholipases C and D is an early response to a cold exposure in Arabidopsis suspension cells. *Plant Physiol.* **130**, 999-1007.

Sanchez, J.P., & Chua, N.H. (2001). Arabidopsis PLC1 is required for secondary responses to abscisic acid signals. *Plant Cell* **13**, 1143-1154.

Sengupta, S., Mukherjee, S., Basak, P., & Majumder, A.L. (2015). Significance of galactinol and raffinose family oligosaccharide synthesis in plants. *Front Plant Sci* **6**, 1-11.

Shears, S. B. (2009). Diphosphoinositol polyphosphates: metabolic messengers? *Mol. Pharmacol.* **76**, 236-252.

Siegel, R.S., Xue, S., Murata, Y., Yang, Y., Nishimura, N., Wang, A., *et al.* (2009). Calcium elevation-dependent and attenuated resting calcium-dependent abscisic acid induction of stomatal closure and abscisic acid-induced enhancement of calcium sensitivities of S-type anion and inward-rectifying K channels in Arabidopsis guard cells. *Plant J.* **59**, 207-220.

Song, M., Liu, S., Zhou, Z., & Han, Y. (2008). *TfPLC1*, a gene encoding phosphoinositide-specific phospholipase C, is predominantly expressed in reproductive organs in *Torenia fournieri*. *Sex. Plant Repro.* **21**, 259-267.

Stevenson-Paulik, J., Bastidas, R. J., Chiou, S.-T., Frye, R. a, & York, J.D. (2005). Generation of phytate-free seeds in Arabidopsis through disruption of inositol polyphosphate kinases. *Proc. Natl. Acad. Sci. USA* **102**, 12612-12617.

Stevenson, J. M., Perera, I.Y., Heilmann, I., Persson, S., & Boss, W.F. (2000). Inositol signaling and plant growth. *Trends Plant Sci* **5**, 252-258.

Sui, Z., Niu, L., Yue, G., Yang, A., & Zhang, J. (2008). Cloning and expression analysis of some genes involved in the phosphoinositide and phospholipid signaling pathways from maize (*Zea mays* L.). *Gene* **426**, 47-56.

Takahashi, S., Katagiri, T., Hirayama, T., Yamaguchi-Shinozaki, K., & Shinozaki, K. (2001). Hyperosmotic stress induces a rapid and transient increase in inositol 1,4,5-trisphosphate independent of abscisic acid in Arabidopsis cell culture. *Plant Cell Physiol.* **42**, 214-222.

Tan, X., Calderon-Villalobos, L.I., Sharon, M., Zheng, C., Robinson, C. V, Estelle, M. *et al.* (2007). Mechanism of auxin perception by the TIR1 ubiquitin ligase. *Nature* **446**, 640-645.

Tasma, I.M., Brendel, V., Whitham, S., & Bhattacharyya, M.K. (2008). Expression and evolution of the phosphoinositide-specific phospholipase C gene family in *Arabidopsis thaliana*. *Plant Physiol. Biochem.* **46**, 627-637.

Testerink, C., & Munnik, T. (2005). Phosphatidic acid: a multifunctional stress signaling lipid in plants. *Trends Plant Sci.* **10**, 368-375.

Tetyuk, O., Benning, U.F. & Hoffmann-Benning, S. (2013). Collection and analysis of Arabidopsis phloem exudates using the EDTA-facilitated method. *J. Vis. Exp.* **80**, e51111.

Tripathy, M.K., Tyagi, W., Goswami, M., Kaul, T., Singla-Pareek, S.L., Deswal, R., *et al.* (2011). Characterization and functional validation of tobacco PLCδ for abiotic stress tolerance. *Plant Mol. Biol. Rep.* **30**, 488-497.

van den Ende, W. (2013). Multifunctional fructans and raffinose family oligosaccharides. *Front. Plant Sci.* **4**, 1-11.

van Leeuwen, W., Vermeer, J.E.M., Gadella, T.W.J., & Munnik, T. (2007). Visualization of phosphatidylinositol 4,5-bisphosphate in the plasma membrane of suspension-cultured Tobacco BY-2 cells and whole Arabidopsis seedlings. *Plant J.* **52**, 1014-26.

Vermeer, J.E.M., Thole, J.M., Goedhart, J., Nielsen, E., Munnik, T., & Gadella, T.W.J. (2009). Imaging phosphatidylinositol 4-phosphate dynamics in living plant cells. *Plant J.* **57**, 356-372.

Vermeer, J.E.M., van Leeuwen, W., Tobeña-Santamaria, R., Laxalt, A.M., Jones, D.R., Divecha, N., *et al.* (2006). Visualization of PtdIns3P dynamics in living plant cells. *Plant J.* **47**, 687-700.

Vermeer, J.E.M, van Wijk R, Goedhart J., Geldner N., Chory J., Gadella Jr. T.W.J. (2017) Imaging diacylglycerol in the cytosolic leaflet of plant membranes. *Plant Cell Physiol.* **58**, 1196-1207.

Vossen, J.H., Abd-El-Haliem, A., Fradin, E.F., Van den Berg, G.C.M., Ekengren, S. K., Meijer, H.J.G., *et al.* (2010). Identification of tomato phosphatidylinositol-specific phospholipase-C (PI-PLC) family members and the role of PLC4 and PLC6 in HR and disease resistance. *Plant J.* **62**, 224-239.

Wang, C.-R., Yang, a.-F., Yue, G.-D., Gao, Q., Yin, H.-Y., & Zhang, J.-R. (2008). Enhanced expression of phospholipase C 1 (*ZmPLC1*) improves drought tolerance in transgenic maize. *Planta* **227**, 1127-1140.

Wheeler, G.L., & Brownlee, C. (2008). Ca^{2+} signaling in plants and green algae-changing channels. *Trends Plant Sci.* **13**, 506-514.

Winter D, Vinegar B, Nahal H, Ammar R, Wilson GV, Provart NJ (2007) An "electronic Fluorescent Pictograph" browser for exploring and analyzing large-scale biological data sets. *PLoS ONE* **2**, e718

York, J.D. (2006). Regulation of nuclear processes by inositol polyphosphates. *Biochim. Biophys. Acta* **1761**, 552-559.

Zhang, J., Vanneste, S., Brewer, P.B., Michniewicz, M., Grones, P., Kleine-Vehn, J., *et al.* (2011). Inositol trisphosphate-induced Ca^{2+} signaling modulates auxin transport and pin polarity. *Develop. Cell* **20**, 855-866.

Zheng, S., Liu, Y., Li, B., Shang, Z., Zhou, R., & Sun, D. (2012). Phosphoinositide-specific phospholipase C9 is involved in the thermotolerance of Arabidopsis. *Plant J.* **69**, 689-700.

Zhu, J. (2016). Abiotic stress signaling and responses in plants. *Cell* **167**, 313-324.

Zonia, L., & Munnik, T. (2004). Osmotically induced cell swelling versus cell shrinking elicits specific changes in phospholipid signals in tobacco pollen tubes. *Plant Physiol.* **134**, 813-823.

Zonia, L., Cordeiro, S., Tupý, J., Feijó, J.A. (2002) Oscillatory chloride efflux at the pollen tube apex has a role in growth and cell volume regulation and is targeted by inositol 3,4,5,6-tetrakisphosphate. *Plant Cell* **14**, 2233-2249.

Figure legends

Fig. 1. Knock-down mutants of *PLC3* exhibit mild defects in primary root growth and lateral root development.

(A) *PLC3* gene and position of T-DNA insertions *plc3-2* and *plc3-3*. Filled boxed and lines represent exons and introns, respectively. Open, grey boxes and triangle represent untranslated region, X- and Y-domains and T-DNA insertions, respectively. (B) Confirmation of reduced *PLC3* expression in *plc3* lines by cDNA amplification. *PLC3*-specific primers were used to detect *PLC3* mRNA by RT-PCR. *TUBULINα4* (*TUB*) was used as loading control. (C) Q-PCR analysis showing *PLC3* expression levels in wild-type and *plc3-2* and *plc3-3*. Relative expression is based on the expression of the *SAND* gene. Values are means ± SD (n = 3) for one representative experiment. (D) Seedling morphology of wild-type and *plc3* mutants. Seeds were germinated on ½ MS with 0.5% sucrose for 4 days, then transferred to ½MS plates without sucrose. Photographs were taken 12 days after germination (DAG). (E) Primary root (PR) length, lateral root (LR) number and lateral root (LR) density at 12 DAG showing reduced numbers for *plc3* mutants. Values are means ± SE of three independent experiments (n>20). Asterisk (*) indicate significance at $P<0.05$ compared to WT based on Student's *t* test.

Fig. 2. Expression pattern of *PLC3.*

cDNA for GUS was cloned in frame of the *PLC3* promoter and introduced into *Arabidopsis*. GUS was expressed throughout *Arabidopsis* plants, predominantly in the vasculature of 2-d old- (A) and 10-d old seedlings, including, shoot and root (B-I). GUS activity was also typically detected in vascular tissue of mature plants (J), trichome base (indicated by arrows) (J, K), hydathodes (J), silique (L), developing seed chalaza (M) and different parts of the flower (N), including style, filament, receptacle and pedicel (indicated by arrows). Experiments were repeated at least two times with similar results.

Fig. 3. Seeds of *PLC3* loss-of-fuction mutants exhibit delayed germination rates and are less sensitive to ABA inhibition of germination.

(A) Seed-germination rate was determined by radical emergence and scored in WT and *plc3* mutants. Seeds were stratified on ½MS with 0.5% sucrose plates at 4°C for 2 days and allowed to germinate at 22°C. Data shown are the means ± SD for a representative experiment (n=55 seeds for each genotype), that was repeated twice with similar results. Asterisks (*) mark that *plc3* values are significantly different from WT based on Student's *t-test* ($P< 0.05$). (B) Histochemical analyses of germinating pPLC3::GUS seeds. GUS activity was detected in embryo cotyledons during seed germination from testa rupture until radical emergence (20-28hrs after transfer from 4°C to 22°C). This experiment was repeated twice with similar outcome. (C) Seeds germination rate of wild-type and *plc3* mutants in the presence or absence of 1- (*left*) or 2 μM ABA (*right*). Seeds were germinated on ½MS with 0.5%

sucrose plates with different concentration of ABA at 22 °C after 2 days of stratification at 4 °C. Germination is defined by radical emergence and was scored at the indicated times. Data shown are the means ± SD from one representative experiment of at least 3 experiments (n=55 seeds for each genotype). Asterisks (*) mark that *plc3* value are significantly different from wild-type based on Student's *t-test* ($P < 0.05$). This experiment was repeated three times with similar results.

Fig. 4. Knock-down *PLC3* mutants exhibit reduced sensitivity to ABA induced-stomatal closure.
(A) Histochemical GUS analysis of epidermal leaf peels of three weeks-old p*PLC3::GUS* plants, showing expression in guard cells. (B) Effect of ABA on stomatal aperture in wild-type (WT), *plc3-2* (left panel) or *plc3-3* (right panel). Epidermal strips were incubated in opening buffer in the light for 3h until stomata were fully open. Strips were then incubated for 90 mins with ABA for the concentrations indicated, after which the stomata were digitized and the aperture width measured. Data was analyzed by 2-way ANOVA. Statistically significant differences between genotypes are indicated by letters ($P<0.05$, Dunn's method). Values are means ± SE of at least three independent experiments ($n \geq 100$).

Fig. 5. PPI- and PA levels in germinating seeds of wild-type and *plc3* mutants and the effect of ABA.
Seeds of wild-type and *plc3* mutants were pre-germinated on ½ MS with 0.5% sucrose plates until testa ruptured and then labeled for 24 h with $^{32}P_i$ and the last two hrs treated with buffer ± 100 μM ABA. (A) Autoradiograph of a typical experiment, with each lane representing the extract of ± 200 seeds. (B) Quantification of the ^{32}P-levels of PIP_2, PIP and PA. Three independent experiments were performed; data shown are means ± SD (n=3) from one representative experiment. Data was analyzed by 2-way ANOVA. Statistical significant differences between genotypes are indicated by letters ($P<0.05$, Dunn's method).

Fig. 6. PPI- and PA levels in leaf peels and effect of ABA in wild-type and *plc3* mutants.
Three-week-old rosette leaf peels from wild-type and *plc3* mutants were $^{32}P_i$-labeled for 3h and then treated in buffer ± 100 μM ABA for 15 min. Lipids were then extracted and separated by TLC. Radioactivity levels in PIP_2, PIP and PA were determined as percentage of total phospholipids. Three independent experiments were performed. Data shown are the means ± SD (n=3) from one representative experiment. Data was analyzed by 2-way ANOVA. Statistical significant differences between genotypes are indicated by letters ($P<0.05$, Dunn's method).

Fig. 7. Overexpression of *PLC3* enhances drought tolerance.
(A) *PLC3* expression levels in wild-type and two homozygous PLC3 overexpression lines, *PLC3-OE9* and *PLC3-OE16* as measured by Q-PCR and based on the expression of the *SAND* reference gene. Values are means ± SD (n = 3) for one experiment. (B) Phenotype of WT - and *PLC3-OE* plants. Four-week old soil-grown plants were exposed to drought stress by water withholding for 2 weeks. (C) Survival rates were determined by counting the visible, green plants after re-watering. (D, E) Fresh- and

dry weights were determined from **shoots** under control and drought (1 week water withholding) conditions. (F) Water loss of detached rosette. Water loss was measured at indicated time points and expressed as a percentage of the initial fresh weight. Values are means ± SD for one representative experiment (n=36). (G) ABA-induced stomatal closure in wild-type, *PLC3 OE9* (left), *PLC3 OE16* (right) plants. Epidermal peels from 3-weeks old plants incubated in opening buffer with light for 3 h until stomata were fully open. Peels were then treated with different concentration of ABA for 90 mins, after which stomata were digitized and the aperture width measured. Values are means ± SE of at least three independents (n >100). Data was analyzed by 2-way ANOVA. Statistical significant differences between genotypes are indicated by letters ($P<0.05$, Dunn's method).

Fig. 8. *PLC3*-overexpression lines exhbit a stronger osmotic-stress induced PIP_2 response.
Six-day-old seedlings were ^{32}P-labeled for 3h and treated with buffer ± 600 mM sorbitol for another 30 min. Lipids were extracted, seperated by TLC and quantified by phosphoimaging. (A) Typical TLC profile with each lane containing $1/5^{th}$ of the extract of 3 seedlings. (B) Quantification of ^{32}P-levels in PIP_2, PIP and PA in wild-type and *PLC3-OE lines #9* and *#16*. Data shown are the means ± SE (n=3) from three independent experiments. Data was analyzed by 2-way ANOVA. Statistical significant differences between genotypes are indicated by letters ($P<0.05$).

Fig. 9. Potential role for PLC in auxin-mediated lateral root formation (A) and ABA-mediated guard-cell signaling (B). For discussion, see text.

Supplementary Material:

Supplemental Methods

Soluble carbohydrates measurement in seeds

Soluble carbohydrates were determined as described by Ribeiro et al. (2014) with minor modifications. Three milligrams of dry seeds were transferred to a 2 mL Eppendorf tube and homogenized in 1 mL of methanol (80% v/v) with the addition of 40 µg of melezitose as internal standard. Samples were incubated in a water bath for 15 minutes at 76°C and dried by vacuum centrifugation. Then, 500 µL of milliQ water was added, thoroughly vortexed and centrifuged for 5 min at 17.000 g in an Eppendorf centrifuge. The supernatant was analyzed with a Dionex HPLC system (ICS 5000 + DC) using a CarboPac PA1, 4 x 250-mm column (Dionex) preceded by a guard column (CarboPac PA1, 4 × 50 mm). Mono-, di-, and trisaccharides were separated by elution in an increasing concentration of NaOH (20-350 mM) with a flow rate of 1 mL per minute. Peaks were identified by coelution of standards.

Phloem sap soluble carbohydrates measurement

Phloem exudates were extracted and analyzed as described earlier (Guelette et al. 2012; Tetyuk *et al*, 2013; modified from Roessner et al. 2000). The hydrophilic fraction (sugars, amino acids, small molecules) was dried and derivatized using methoxyamine in pyridine and BSTFA (N,O-bis-trimethyl-silyltrifluoroacetamide) with 1% trimethylchlorosilane. The metabolites were subsequently separated using an Agilent 5890N GC system, coupled to a 5973 inert MSD using a DB-5MS column (J&W Scientific, 30m x 0.32mm ID x 0.25 µm film; temperature program: 70-5, 5/min-320-5). Identification of compounds occurred using the NIST library (NIST Standard Reference Database; https://www.nist.gov/srd/nist-standard-reference-database-1a-v14) in combination with co-elution of standards. Peak area determination was performed using QuanLynx, a quantification software within the MassLynx software (Waters). The experiment was repeated five times.

Supplemental Figure legends

Supplemental Table S1. Primers for the identification of *PLC3* T-DNA insertion mutants and for *PLC3* RT-PCR.

Supplemental Figure S1. Segmented-*PLC3* expression correlates with lateral root formation. $PLC3_{pro}$*:GUS-YFP* seedlings were grown on ½MS agar plates under normal conditions (see Material & Methods) and stained for GUS activity after 10 days. Typically, roots were not homegenously stained but revealed a segmnented pattern that correlated with lateral root formation. Numbers indicate the magnification of the objective by which the pictures were made.

Supplemental Figure S2. *PLC3$_{pro}$:GUS-YFP* expression in seedlings grown at 45° angle.
To find a stronger correlation between lateral root formation and the segmented PLC3-GUS expression, seedlings were grown for 10 days on ½MS agar plates at an angle of 45° in stead of the common 80° angle (*e.g.* Supplemental Fig 1). This lower angle results in a more wiggled growth of the primary root, which forces later roots to form at the designated, 'curved' sites. (A) Cartoon of the setup. (B) Cartoon of the curvy seedlings generated and the lateral root formation at the curved sites (indicated by blue circles). (C) Histological GUS analysis of *PLC3$_{pro}$:GUS-YFP* seedlings grown for 10-d at a 45° angle. Using this setup, less segments without lateral root were found (red circles). It emphasises that *PLC3* expression is not homogenous throughout the root vasculature: going from segmented (top), to complete GUS-possitive (middle) to no GUS activity (root tip, transition zone).

Supplemental Figure S3. Confocal analysis of *PLC3$_{pro}$:GUS-YFP* expression. Confocal image of longitudinal section (A) and cross section (B) of 5-d old seedlings. (C) eFP browser database of *PLC3* expression in old and young root tissues.

Supplemental Figure S4. Effect of ABA on phospholipid-signaling responses in *Arabidopsis* WT- and *plc3* seedlings.
(A-D) Time-course of ABA response in WT seedlings. Six-day-old seedlings were $^{32}P_i$-labeled for 3h and then treated with buffer with or without 100 µM ABA for different periods of time (0, 2, 4, 8, 16, 32 and 64 min). Lipids were extracted and separate by TLC. Radioactivity was visualized by autoradiography (A) and quantified by phosphoimaging (B-D). Lipids are expressed as fold-increase with respect to control. Values are the means of triplicates ± SD for one representative experiment. Data was analyzed by 2-way ANOVA. Statistical significant differences between genotypes are indicated by letters ($P<0.05$, Dunn's method).
(E-H) ABA response in *plc3* mutants. Five-day-old WT- and *plc3* seedlings were $^{32}P_i$-labeled for 3h and then treated with buffer or 100 µM ABA for 1 h. (E) Autoradiograph of TLC. (F-H) Quantification of PIP_2, PIP and PA. Data shown are the means ± SE of three independent experiments. Data was analyzed by 2-way ANOVA. Statistical significant differences between genotypes are indicated by letters ($P<0.05$, Dunn's method).

Supplemental Figure S5. Shorter primary root in *plc3* mutants is due to delayed germination.
(A) Primary root lengths of WT and *plc3* mutants were determined on day 4, 6, 8 and 10. (B) Relative root growth between day 6 and 4, day 8 and 4, and day 10 and 4. Values are means ± SD of a representative experiment ($n>20$).

Supplemental Figure S6. Effect of ABA on root development in wild-type and *plc3* mutants.
(A) Seedling morphology of wild-type and *plc3* under normal and ABA conditions. Seeds were germinated on ½MS with 0.5% sucrose for 4 days and then transferred to ½MS ± 10 µM ABA.

Photographs were taken 12 d after germination. (B) Relative primary root- (PR-) and lateral root (LR) elongation were calculated as a percentage of the length under control condition. Three independent experiments were performed. Data shown are the means ± SD (n>10) for one representative experiment.

Supplemental Figure S7. Drought tolerance is not affected in *plc3* mutants.

Phenotype of six-week-old wild-type, *plc3-2* and *plc3-3* plants with or without two weeks of drought. Three independent experiments were performed (A-C) and in neither case, differences between WT and *plc3* mutants were found. Four-week old soil-grown plants were exposed to drought stress by water withholding for 2 weeks and then photographed. Control plants were normally watered during that period.

(A) Setup with five- or nine plants per pot. The latter experienced drought earlier. Top- and side views are shown.

(B) Setup with eight plants per pot, four pots per tray, six trays in total (192 plants). For control condition, two trays (64 plants) were used.

Supplemental Figure S8. Relative water content (RWC) of WT- and *PLC3-OE* rosettes under control- and drought conditions.

Fresh weight (FW) of the rosettes were measured directly after cutting. To determine the turgid weight (TW) the rosette was placed O/N on water at 4°C in the dark and weighted. The dry weight (DW) was recorded after oven-drying at 65°C for 48 h. RWC was calculated as RWC $(\%) = [(FW - DW) / (TW - DW)] \times 100$. Values are means ± SE (n>20). Data was analyzed by 2-way ANOVA. Statistical significant differences between genotypes are indicated by letters (P<0.05).

Supplemental Figure S9. Soluble sugar composition in seeds or phloem sap is not affected in *plc3* mutants.

(A) Soluble sugar composition in seeds. Sugars were extracted from dry seeds and analyzed by Dionex HPLC. Sugar quantities were corrected by means of an internal standard and transformed to µg of sugar per mg of dry material. Values are the means of triplicates ± SE of three independent seed batches. (B) Phloem sugar composition. Phloem sap was isolated from 6-week-old Arabidopsis plants and their sugars analyzed and quantified by GC-MS. Values are the means of triplicates ± SD from 3 independent experiments.

Supplemental Figure S10. PPI-, PA- and IPP levels in WT and *plc3*-seedlings

(A-B) ^{32}P-Lipid levels in wt and *plc3* seedlings (C-F) ^{3}H-IPP levels in WT and *plc3*-mutant seedlings labeled in two distict ways. For (C, D), eleven-day old seedlings were labeled with ^{3}H-*myo*-inositol for 7 days whereas for (E, F), four-days old seedlings were labeled for 4 days. Extracted IPPs were resolved by HPLC-SAX chromatography and the radioactivity in the fractions determined by liquid

scintillation counting. The quantities are expressed as percentage of total. (D) ^{3}H-IP$_8$ levels. (F) ^{3}H-IP$_7$ levels. (C, D) represents the means ± SD (n=10) of one representative experiment with similar results obtained in an independent experiment, whereas (E, F) show means ± SE (n=10) from three independent experiments.

Supplemental Figure S11. Gravitropic-root response of *plc3*-mutant seedlings is not affected

(A, B) Seedlings were grown on ½MS with 0.5% sucrose plate for 4 days, afterwhich plates were rotated by 90° and photographed 2 days after turning (6-d old seedling). (C) Bending was expressed as curvature angle. Values are means ± SD for one representative experiment (n>20). This experiment was repeated twice with similar results.

Figure 1 – Zhang *et al.*

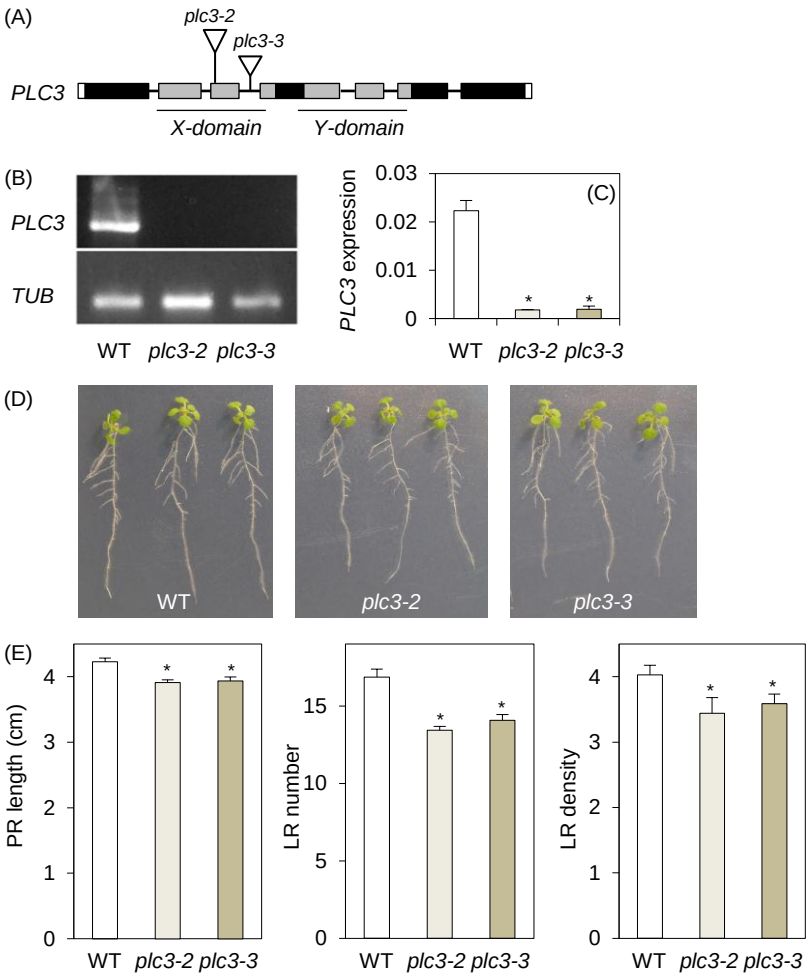

Figure 2 – Zhang *et al.*

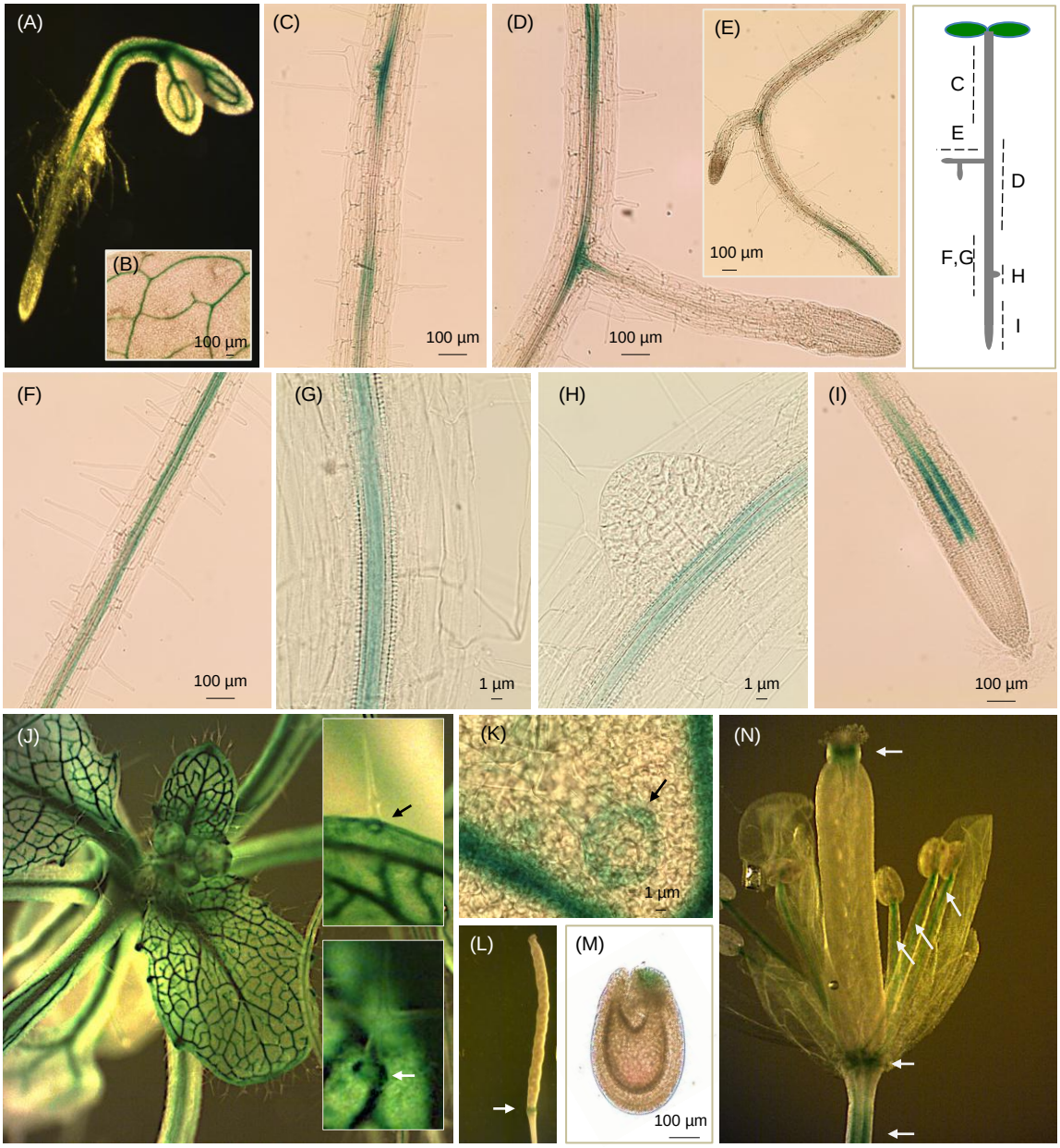

Figure 3 – Zhang *et al.*

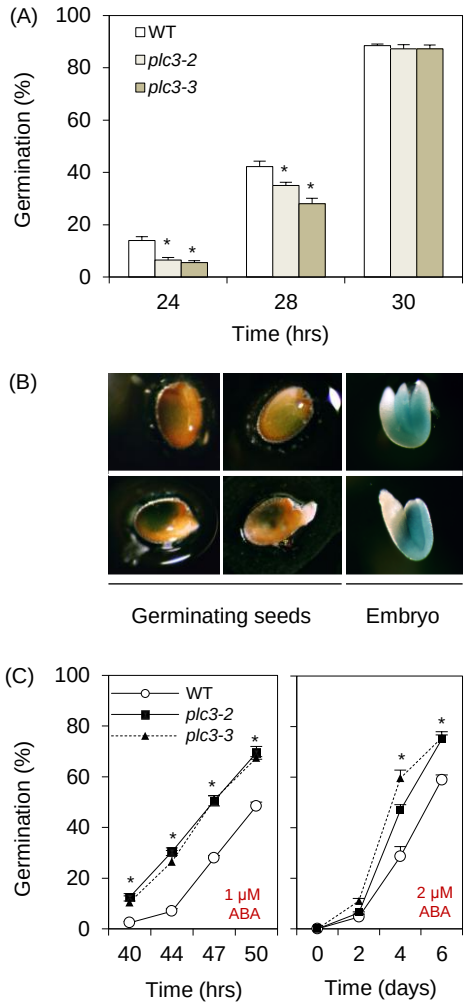

Figure 4 – Zhang *et al.*

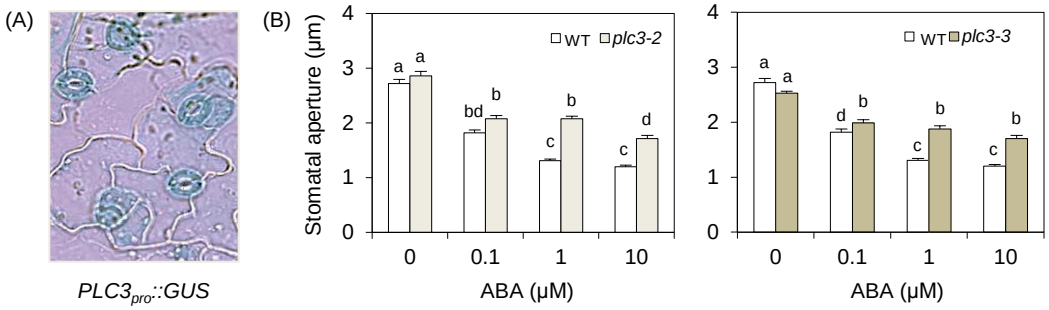

PLC3$_{pro}$*::GUS*

Figure 5 – Zhang *et al.*

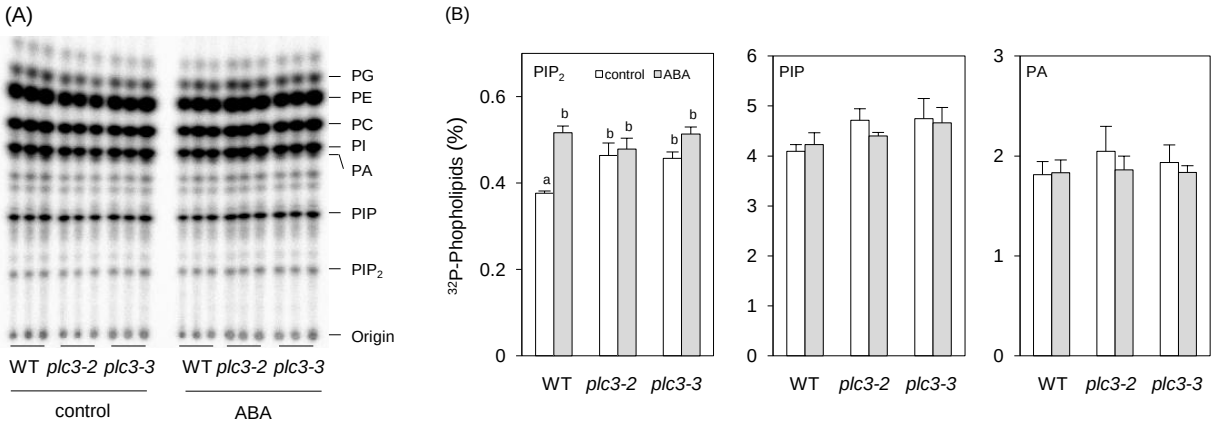

Figure 6 – Zhang *et al.*

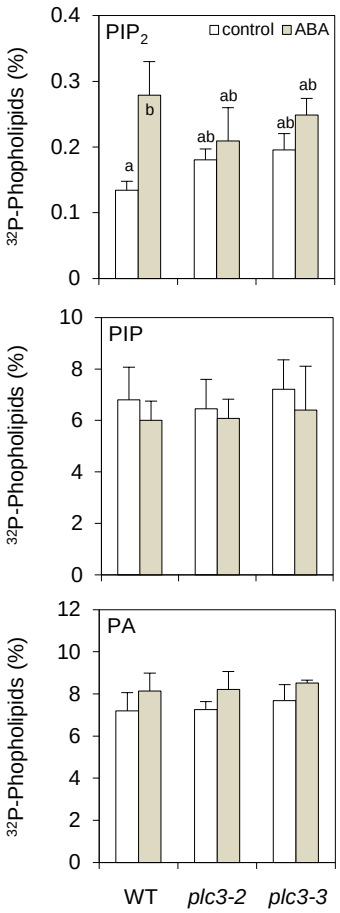

Figure 7 – Zhang *et al.*

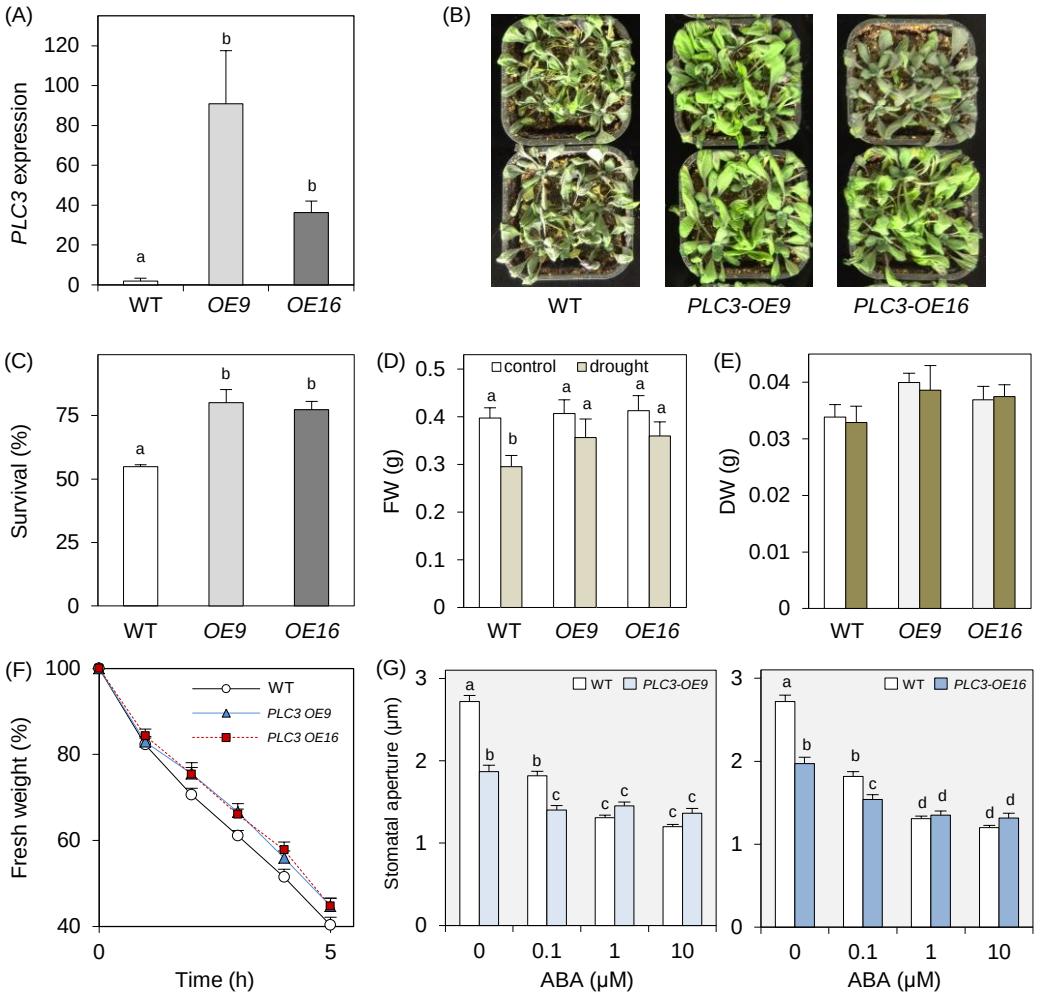

Figure 8 – Zhang *et al.*

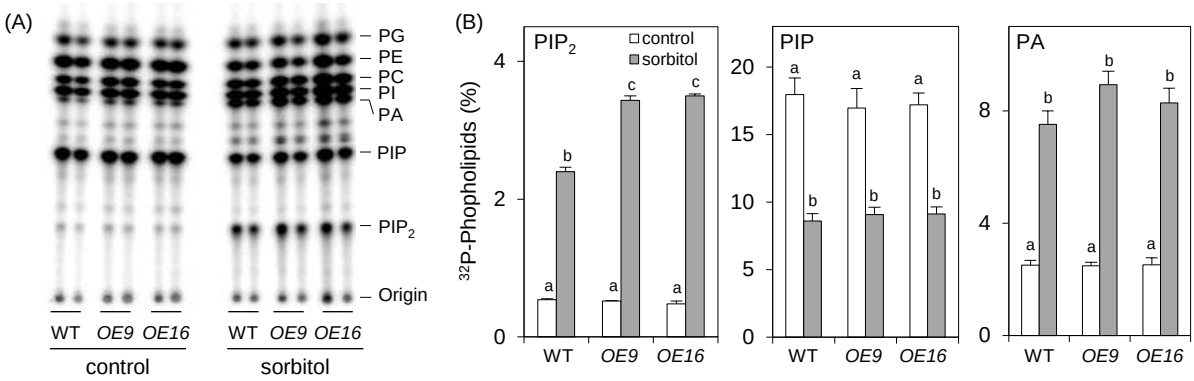

Figure 9 – Zhang *et al.*